

AD/A-003 595

INVESTIGATION OF THE EXPLOSIVE POTENTIAL
OF THE HYBRID PROPELLANT COMBINATIONS
N₂O₄/PBAN AND CTF/PBAN

C. Wilton

URS Research Company

Prepared for:

Air Force Rocket Propulsion Laboratory

March 1967

DISTRIBUTED BY:

NTIS

National Technical Information Service
U. S. DEPARTMENT OF COMMERCE

540
AD A 0 0 3 5 9 5

1

Reproduced by
NATIONAL TECHNICAL
INFORMATION SERVICE
US Department of Commerce
Springfield, VA. 22151

URS
CORPORATION

PRICES SUBJECT TO CHANGE

DISTRIBUTION STATEMENT A
Approved for public release
Distribution Unlimited

DDC
RECEIVED
JAN 24 1975
D

URS 652-26

INVESTIGATION OF THE EXPLOSIVE POTENTIAL OF THE HYBRID
PROPELLANT COMBINATIONS N_2O_4 /PBAN AND CTF/PBAN

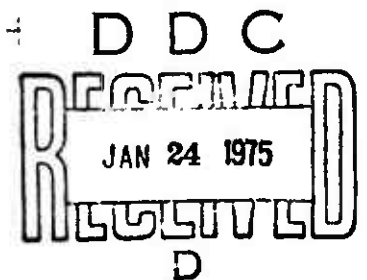
March 1967

Technical Documentary Report No. AFRPL-TR-67-124

Prepared under Contract No. AF 04(611)-10739

by

URS CORPORATION
1811 Trousdale Drive
Burlingame, California



for

AIR FORCE ROCKET PROPULSION LABORATORY
Research and Technology Division
Air Force Systems Command
United States Air Force
Edwards, California

DISTRIBUTION STATEMENT A

Approved for public release;
Distribution Unlimited

ABSTRACT

The Air Force Rocket Propulsion Laboratory (AFRPL), with assistance from URS Corporation, has conducted a limited program to determine the explosive potential of two hybrid propellant combinations; nitrogen tetroxide (N_2O_4) and polybutadiene-aluminum (PBAN), and chlorine trifluoride (CTF) and PBAN. This program consisted of a series of eight tests in which the N_2O_4 /PBAN propellant combination was subjected to high-velocity impact tests, drop tests, and explosive-donor tests, and one high-velocity impact test of the CTF/PBAN propellant combination.

The test program design, test hardware, tankage and instrumentation systems and the blast and thermal data from each of the test series are described in this report.

Explosive yields obtained for the N_2O_4 /PBAN propellant combination (using TNT as a reference explosive) were: 0.4% for the flat-wall high-velocity impact test and 1 to 4% for the deep-hole high-velocity impact tests; 5 to 13% for the various types of explosive-donor tests and < 0.01% for the tower drop tests. The explosive yield for the CTF/PBAN deep-hole high-velocity impact test was < 1%.

FOREWORD

This report, which was prepared by the URS Corporation, Burlingame, California, on Air Force Contract AF 04(611)-01739, presents the results from a limited program to determine the explosive potential of two hybrid propellant combinations; nitrogen tetroxide (N_2O_4) and polybutadyne - aluminum (PBAN) and chlorine trifluoride (CTF) and PBAN.

This program was initiated in May 1966 under the direction of Mr. Austin A. Dickinson, the AFRPL Project Engineer. URS Corporation, with Mr. C. Wilton as Principal Investigator, has provided analytical services and consultation on experimental design. Mr. J. Mansfield was an associated URS Project Engineer.

This report has been reviewed and approved.



AUSTIN A. DICKINSON
Project Engineer, Hybrid Hazard Program
Solid Rocket Division
Air Force Rocket Propulsion Laboratory

CONTENTS

<u>Section</u>	<u>Page</u>
FOREWORD	ii
GLOSSARY OF EXPLOSIVE AND BLAST WAVE TERMS	viii
1 INTRODUCTION	1-1
2 TEST PROGRAM DESIGN	2-1
High-Velocity Impact	2-2
Explosive Donor	2-2
Tower Drop	2-3
3 N ₂ O ₄ /PBAN HIGH-VELOCITY-IMPACT-TEST SERIES	3-1
Introduction	3-1
Tankage for the High-Velocity-Impact Test Series	3-1
High-Velocity-Impact Targets	3-3
Instrumentation System	3-11
Test Results	3-11
4 N ₂ O ₄ /PBAN EXPLOSIVE-DONOR AND DROP-TEST SERIES	4-1
Tankage for the Explosive-Donor Test Series	4-1
Drop Test Tanks	4-4
Instrumentation System	4-4
Test Results	4-9
Thermal Measurements	4-14
5 CTF/PBAN HIGH-VELOCITY-IMPACT-TEST	5-1
6 DISCUSSION OF RESULTS	6-1
N ₂ O ₄ /PBAN Tests	6-1
CTF/PBAN Test	6-3
Comparison with Hypergolic Results	6-3
Appendix A	
DESCRIPTION OF N ₂ O ₄ /PBAN TESTS	A-1

ILLUSTRATIONS

<u>Figure</u>		<u>Page</u>
1	Hybrid Impact Tank	3-2
2	Hydrazine Container	3-4
3	N_2O_4 /PBAN High-Velocity-Impact Tank	3-5
4	N_2O_4 /PBAN High-Velocity-Impact Tank and Propulsion Unit . . .	3-6
5	Flat-Wall Target	3-7
6	Flat-Wall Target	3-8
7	Deep-Hole Target	3-9
8	Deep-Hole Target	3-10
9	Test Site and Instrumentation Layout for High-Velocity Impact Tests	3-12
10	Typical Gauge Mount	3-13
11	Peak Overpressure vs Scaled Ground Distance for High-Explosive Calibration Tests	3-16
12	Positive Phase Impulse vs Scaled Ground Distance for High-Explosive Calibration Tests	3-17
13	Sketch Indicating Differences Between Full-Scale and Test Geometry	3-22
14	Plots Showing Method of Extrapolation to Obtain 0-Deg Yield Values (see Text)	3-23
15	N_2O_4 /PBAN Explosive-Donor Tank	4-2
16	N_2O_4 /PBAN Explosive Donor Tank with 30 lb Donor in Place . . .	4-3
17	Sketch of N_2O_4 /PBAN Drop Tank	4-5
18	Sketch of the Drop Tower	4-6
19	Instrumentation Layout	4-8
20	Type A Sensor Mount	4-10
21	Type B Sensor Mount	4-11

ILLUSTRATIONS (Cont)

<u>Figure</u>		<u>Page</u>
22	Type C Sensor Mount	4-12
23	Radiant Intensity vs Time at Locations Outside the Fireball from Test 243	4-21
24	Stainless Steel Slab Surface Temperature and Radiant Intensity Located 10 ft from Ground Zero Along Gauge Line A for Test 243	4-22
25	Slab Surface Temperature for Test 243	4-23
26	CTF/PBAN High-Velocity-Impact Tank	5-2
27	CTF/PBAN Propellant Tank in Place on Test Track	5-3
28	Rear View of CTF/PBAN Propellant Tank Showing PBAN Propellant .	5-4
29	Post-Slot Photo N_2O_4 /PBAN Deep-Hole Target	5-5
A-1	Schematic of K-2 Terminal Ballistic Range	A-2
A-2	N_2O_4 /PBAN High-Velocity-Impact Tank	A-3
A-3	N_2O_4 /PBAN High-Velocity-Impact Tank and Propulsion Unit	A-4
A-4	Flat-Wall Target	A-5
A-5	Deep-Hole Target	A-6
A-6	Pre-Test Photo, Test Number 2	A-7
A-7	Post-Test Photo, Test Number 3	A-9
A-8	Post-Test Photo, Test Number 4	A-10
A-9	Post-Test Photo, Test Number 5	A-11
A-10	Pre-Test Photo, Test Number 6	A-12
A-11	Pre-Test Photo, Test Number 7	A-13
A-12	Post-Test Photo, Test Number 7	A-14
A-13	Liquid Propellant Hazard Test Stand and Tower	A-15
A-14	Pre-Test Photo, Test Number 243	A-17

ILLUSTRATIONS (Cont)

<u>Figure</u>		<u>Page</u>
A-15	Pre-Test Photo, Test Number 244	A-18
A-16	Post-Test Photo, Test Number 244	A-19
A-17	Pre-Test Photo of Test Article Used for Test Number 260	A-20
A-18	Post-Test Photo, Test Number 260	A-21
A-19	Post-Test Photo, Test Number 260	A-22
A-20	Test Article used for Test Number 261	A-23
A-21	Post-Test Photo, Test Number 261	A-24
A-22	Post-Test Photo, Test Number 261	A-25
A-23	Post-Test Photo, Test Number 261	A-26

TABLES

<u>Table</u>		
1	Summary of Tests for N ₂ O ₄ /PBAN High-Velocity-Impact-Test Series	3-14
2	Peak Overpressure and Positive-Phase-Impulse Data from High-Explosive Calibration Tests 2 and 7	3-15
3	Peak Overpressure and Positive-Phase-Impulse data From N ₂ O ₄ /PBAN High-Velocity Impact Tests	3-19
4	Explosive Yields from N ₂ O ₄ /PBAN High Velocity Impact Tests	3-20
5	Terminal Yields from N ₂ O ₄ /PBAN High-Velocity-Impact Tests	3-24
6	Instrumentation Layout at AFRPL	4-7
7	Summary of Test Conditions for N ₂ O ₄ /PBAN Explosive-Donor and Drop-Test Series.	4-13
8	Peak Overpressure and Positive Phase-Impulse Data from N ₂ O ₄ /PBAN Explosive Donor Test	4-15
9	Terminal Yields from N ₂ O ₄ /PBAN Explosive Donor Tests.	4-16
10	Thermal Data.	4-19-20

TABLES (Cont)

<u>Table</u>		<u>Page</u>
10	Peak Overpressure and Positive-Phase Impulse Data from CTF/PBAN Propellant Test	5-6
11	Explosive Yields from CTF/PBAN High-Velocity-Impact Test Adjusted to TNT.	5-7
12	Summary of Terminal Yields from N_2O_4 /PBAN Tests	6-2
13	Comparison of Hybrid and Hypergolic Terminal Yields (200-lb Scale)	6-4

GLOSSARY OF EXPLOSIVE
AND BLAST WAVE TERMS

BLAST SCALING LAWS: Scaling laws formulated from the general laws of similitude relating blast and environmental parameters. The most common blast scaling laws (termed "cube root scaling") relate blast wave parameters (e.g., blast pressure P , positive-phase impulse I , and positive-phase duration t^+) to distance from an explosion d , and explosion weight W , as follows:

$$P = f(d/W^{1/3}) = f(\lambda)$$

$$I/W^{1/3} = h(d/W^{1/3}) = h(\lambda)$$

$$t^+/W^{1/3} = g(d/W^{1/3}) = g(\lambda)$$

The quantities $d/W^{1/3}$ and $t^+/W^{1/3}$ are commonly referred to as scaled distance and scaled time, respectively. See SACHS' SCALING LAW.

BLAST WAVE: A pressure pulse (or wave) in air, propagated continuously from an explosion and characterized by an initial generally rapid rise of pressure above ambient values. The air within a blast wave moves in the direction of propagation, causing winds. See SHOCK WAVE.

EXPLOSIVE YIELD: The explosive potential of propellants is usually expressed in terms of their TNT equivalent yield, i.e., the amount of TNT which if put at the position of the propellant explosion would produce the same value of a particular shock wave parameter at the same distance as for the propellant explosion. The explosive yield of a given propellant explosion can be given in equivalent pounds of TNT, although it is more common to express it in terms of the percent of the total weight of propellants involved. The term explosive yield is usually modified by the shock wave parameter used in the calculation, e.g., peak overpressure yield or positive-phase impulse yield.

FREE AIR OVERPRESSURE: (OR FREE FIELD OVERPRESSURE): The unreflected pressure, in excess of the ambient atmospheric pressure, created in the air by the blast wave from an explosion.

IMPULSE (PER UNIT AREA): The integral, with respect to time, of the overpressure in a blast wave at a given point, the integration being carried out between the time of arrival of the blast wave and that at which the overpressure returns to zero at the given point. Impulse dimensions are the product of overpressure and time, e.g., psi-seconds.

OVERPRESSURE: The transient pressure, usually expressed in pounds per square inch, exceeding the ambient pressure, manifested in the shock (or blast) wave from an explosion. The variation of overpressure with time depends on the energy yield of the explosion, the type of explosive or propellant, the distance from the point of burst, and the medium in which the explosive propellants are detonated. The peak overpressure is the maximum value of the overpressure at a given location and is generally experienced at the instant the shock (or blast) wave reaches that location. See SHOCK WAVE.

SACHS' SCALING LAW: Scaling laws relating blast and environmental parameters that include the effects of changes of ambient pressures. These scaling laws are summarized below:

$$P/P_o = f' [d/(W/P_o)^{1/3}] = f' (\lambda')$$

$$I/(W/P_o)^{1/3} = h' [d/(W/P_o)^{1/3}] = h' (\lambda')$$

$$t^+/(W/P_o)^{1/3} = g' [d/(W/P_o)^{1/3}] = g' (\lambda')$$

where P = shock pressure

P_o = ambient pressure

d = distance from the charge

W = charge weight

t^+ = duration of the positive-pressure phase

I = positive-phase impulse

$\lambda' = d/(W/P_o)^{1/3}$

The quantities $d/(W/P_o)^{1/3}$ and $t^+/(W/P_o)^{1/3}$ are commonly referred to as Sachs scaled distance and Sachs scaled time, respectively.

SHOCK FRONT: (OR PRESSURE FRONT): The fairly sharp boundary between the pressure disturbance created by an explosion (in air, water, or earth) and the ambient atmosphere, water, or earth, respectively. It constitutes the front of the shock (or blast) wave.

SHOCK WAVE: A continuously propagated pressure pulse (or wave) in the surrounding medium, which may be air, water, or earth, initiated by the expansion of the hot gases produced in an explosion. A shock wave in air is often referred to as a blast wave. The duration of a shock (or blast) wave is distinguished by two phases. First there is the positive (or compression) phase during which the pressure rises very sharply to a value that is higher than ambient and then decreases to the ambient pressure. The duration of the positive phase increases and the maximum (peak) pressure decreases with increasing

distance from an explosion of a given energy yield. In the second phase, the negative (or rarefaction) phase, the pressure falls below ambient and then returns to the ambient value. Deviations from the ambient pressure during the negative phase are never large. See OVERPRESSURE.

TERMINAL YIELD: The value of the explosive yield in the region where the explosive yield becomes independent of distance from the explosion or the shock wave parameter used in the calculation. See EXPLOSIVE YIELD.

Section 1
INTRODUCTION

The Air Force Rocket Propulsion Laboratory (AFRPL) has conducted a limited program to determine the explosive potential of two hybrid propellant combinations; nitrogen tetroxide (N_2O_4) and polybutadiene-aluminum (PBAN), and chlorine trifluoride (CTF) and PBAN. This program consisted of a series of eight tests in which the N_2O_4 /PBAN propellant combination was subjected to high-velocity-impact tests, drop tests, and explosive-donor tests, and one high-velocity-impact test of the CTF/PBAN propellant combination.

URS Corporation, under Contract AF 04(611)-10739, has provided support for this blast hazard program. This support has included assistance in establishing the design of the program; the design and construction of the test articles; provision of ordnance and instrumentation consulting; reduction and analysis of the test data; and presentation of the results in this report.

A discussion of the rationale behind the design of the test program is presented in Section 2. A description of the test conditions and results from the N_2O_4 /PBAN high-velocity-impact test series are presented in Section 3 and for the N_2O_4 /PBAN drop-test series and high-explosive-donor test series in Section 4. The test condition and results for the CTF/PBAN test are contained in Section 5.

Section 6 presents a comparison of the results from these hybrid propellant combinations with those obtained from tests with the hypergolic propellant combination.

Section 2
TEST PROGRAM DESIGN

For any bipropellant system to give a significant explosive yield in an accidental failure, it is necessary that the failure sequence be such that a significant fraction of one component is finely subdivided and well distributed throughout the other component at or soon after the time of ignition. To achieve this condition for the liquid - solid hybrid combination of concern in this test program means that a sufficiently great mechanical force must be applied to the solid fuel grain during the failure process to cause it to break into small pieces and mix with the liquid component. It would be anticipated, therefore, that significant explosive yields from these propellant combinations, if possible at all, would occur only for rather severe failure conditions.

The situation for the hybrid combinations are somewhat similar to those for hypergolic liquid combinations, which also require rather large mechanical forces to achieve significant explosive yields. In this case large forces are necessary to cause significant mixing before the reaction at the interface between the two components separates them. Because of the similarity between the two cases, the general approach found suitable for evaluating the explosive potential of the hypergolic combination in Project Pyro was also used for the hybrid combinations.

This approach involves a limited program, initially testing the propellant combinations under the most severe failure conditions to determine the maximum possible explosive yields. If these turn out to be negligible, then further testing of less severe conditions is unnecessary. The specific test conditions used were those which had previously been selected (and used) in Project Pyro to provide the greatest mechanical forces. These are:

- High-velocity impact
- Explosive donor
- Tower drop

HIGH-VELOCITY IMPACT

The high-velocity-impact case is intended to simulate nose-on impact a vehicle on the ground surface. A variety of surface targets is appropriate for this case, depending on the nature of the ground surface being simulated. In the Pyro program, these ranged from a flat surface, simulating a rigid ground surface, to a deep hole, simulating a soft surface which would crater on impact. (To avoid simulating the strength characteristics of real vehicles, the soft-surface-cratering condition was achieved by using a preformed crater in a rigid material.) This deep-hole target gave the largest explosive yields for both hypergolic and cryogenic propellant combinations, so this target geometry was also selected for the hybrid tests. The specific geometry used was a cylindrical hole with a depth three times the radius. An impact velocity of 600 fps was selected as a reasonable upper limit obtainable by a high-altitude fallback or powered impact.

EXPLOSIVE DONOR

The explosive-donor case simulates the situation in which the test tankage is subjected to an explosion from an external source. The weight of potential explosive donors can vary over wide limits. However, there are several factors which tend to narrow down the range of primary interest. First, it can be shown that there is not too much concern with donors whose weight approaches that of the propellants. If a donor equal to the propellant weight is necessary to make the majority of the propellants react explosively, then the resulting explosion is not much worse than that given by the donor itself. (An increase in explosive weight by a factor of two only increases the distance at which a given peak pressure is obtained by a factor of $(2)^{1/3}$ or 1.26.)

On the other hand, too small a donor may not be able to cause the propellants to mix and explode (if in fact, they are capable of exploding under the action of an explosive donor). With this line of reasoning, an explosive weight of 30 lb

was selected for the explosive donor, the same as the maximum weight used in the Pyro program for 200-lb propellant quantities.

TOWER DROP

The tower drop case was included to provide another but less severe type of impact test and one which was used in the Pyro program.

In this series, lightweight frangible tanks containing the propellant combinations were dropped from a 101-ft tower, impacting the ground surface at approximately 80 ft/sec.

Section 3

N₂O₄/PBAN HIGH-VELOCITY-IMPACT-TEST SERIES

INTRODUCTION

The high-velocity-impact-test series was conducted by AFRPL at the Naval Ordnance Test Station (NOTS), China Lake. The N₂O₄/PBAN series consisted of three tests, in which tanks containing 200-lb quantities of this propellant combination were propelled down a sled track by solid-motor propulsion units at speeds ranging from 590 to 690 fps and allowed to impact into selected target configurations. These selected target configurations were a flat-wall target and a deep-hole target.

TANKAGE FOR THE HIGH-VELOCITY-IMPACT-TEST SERIES

The criteria for the design of tanks for this series were determined by:

- (1) the requirements to approximately simulate conventional missiles with regard to shape;
- (2) the desirability of using minimum weight, strength, and length-to-diameter ratios consistent with present and expected usage; and
- (3) compliance with the following operational restrictions imposed by NOTS:

- Tanks should be capable of withstanding a 30-G load in any direction
- The liquid-propellant compartment must be pressure tested to 20 psi

A sketch of the tank designed to meet these requirements is presented in Fig. 1. The tanks were cylindrical in shape, 12.8 in. in diameter, 43 in. long, and were fabricated of aluminum. The forward compartment, which contained approximately 120 lb of N₂O₄, had 2:1 ellipsoidal domed ends. These domed ends and the cylindrical walls of the entire tank were of a constant 1/8-in. thickness. Although this is thicker than that calculated by scaling from missile structures,

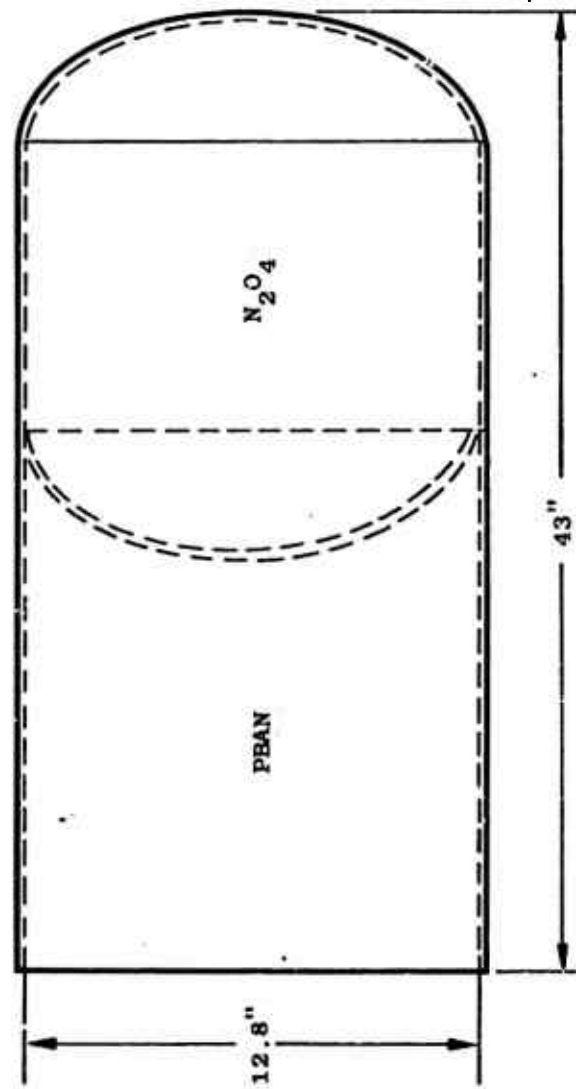


FIG. 1. N_2O_4 /PBAN Hybrid Impact Tank

it is felt to be optimum from the standpoint of tank construction and design load requirements.

The rear compartment of the tank contained approximately 80 lb of solid propellant (PBAN) cast with the following materials; 50.1% PBAN binder, 45% AL-120 Aluminum Power, 3.4% MAPO Catalyst, and 1.5% Cab-o-Sil Powder. This solid propellant was cast in the tank in a "wagon wheel" configuration using a removable wooden mold.

A scaled aluminum cylinder containing 0.5 lb of hydrazine (N_2H_4) was placed in the center core of the solid to simulate the hybrid motor ignition system. This cylinder (pictured in Fig. 2) was 2 in. in diameter and 6.5 in. long and was fabricated from .049-in.-thick aluminum tubing.

Photographs of the high-velocity-impact tank in place, on the K-2 test track are presented in Figs. 3 and 4. Note, in Fig. 3, the location of the hydrazine container in the center perforation of the solid propellant.

HIGH-VELOCITY-IMPACT TARGETS

The flat-wall target configuration consisted of a massive concrete block (weighing approximately 144,000 lb), which was protected by a 4-in.-thick, 6-ft by 10-ft steel facing plate. The flat-wall target, which was placed against this massive block, consisted of a 5/8-in.-thick steel plate, 8 ft high and 16-ft wide, with a 12-in. splash shield around the edge. A sketch of this target is shown in Fig. 5 and pictured in Fig. 6.

For the deep-hole target configuration, the massive concrete block and steel plate was faced with another concrete block, 6 ft in cross section and having a 26-in.-diameter cylindrical cavity 39 in. deep. A sketch of this target geometry is presented in Fig. 7 and pictured in Fig. 8.



Fig. 2. Hydrazine Container.

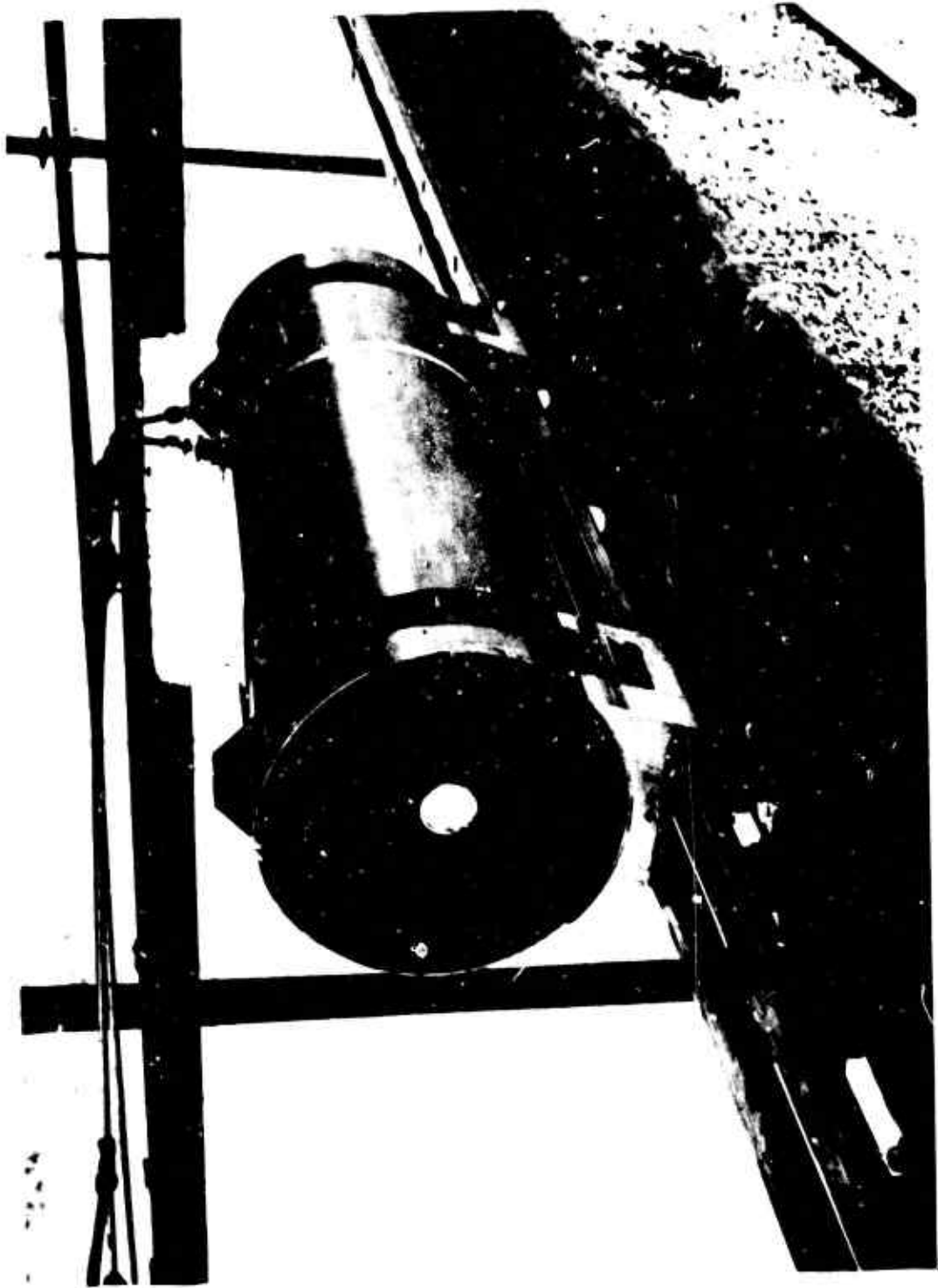


Fig. 3. N_2O_4 /PBAN High-Velocity-Impact Tank

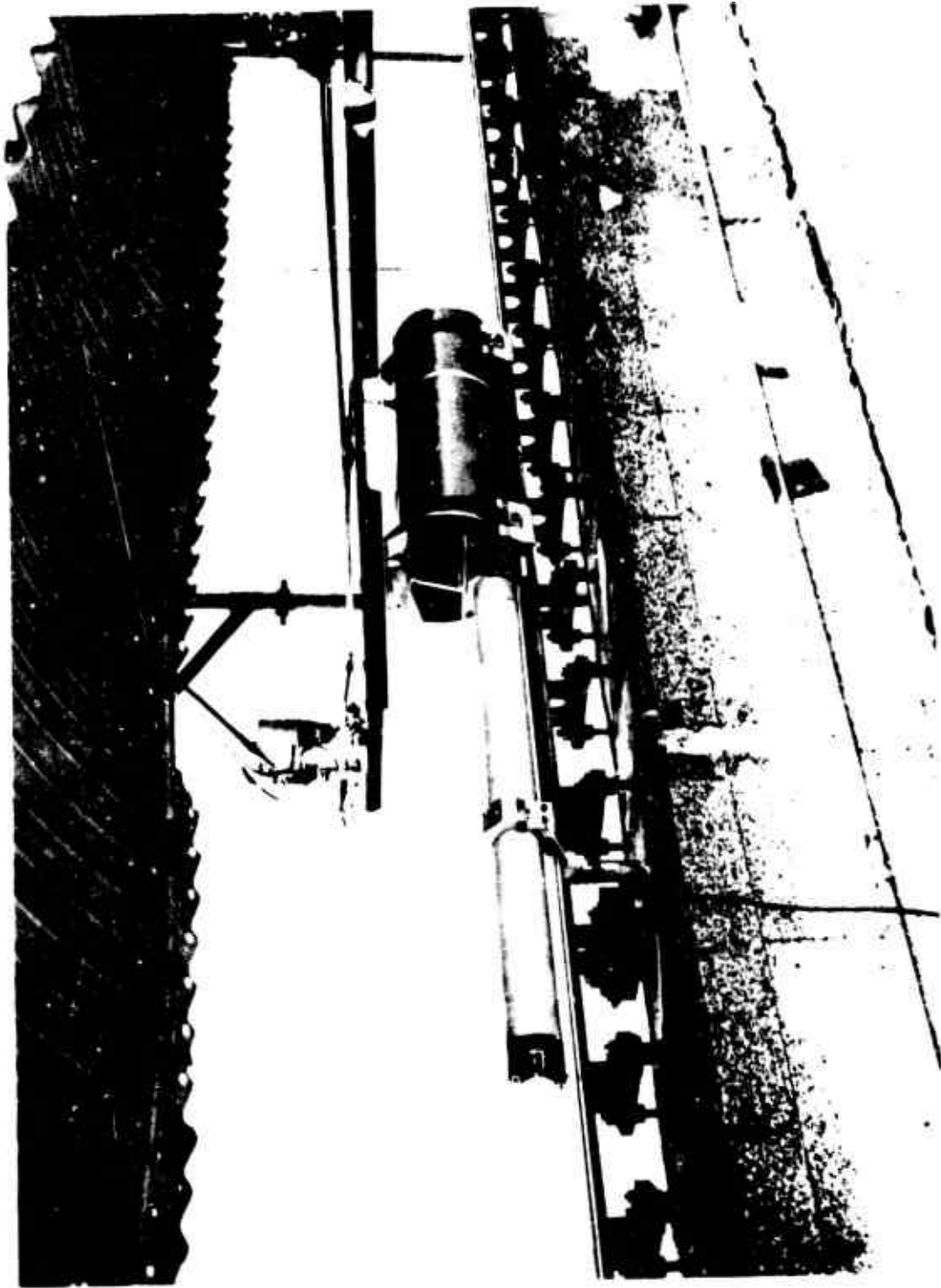


Fig. 4. N_2O_4 /PBAN High-Velocity-Impact Tank and Propulsion Unit.

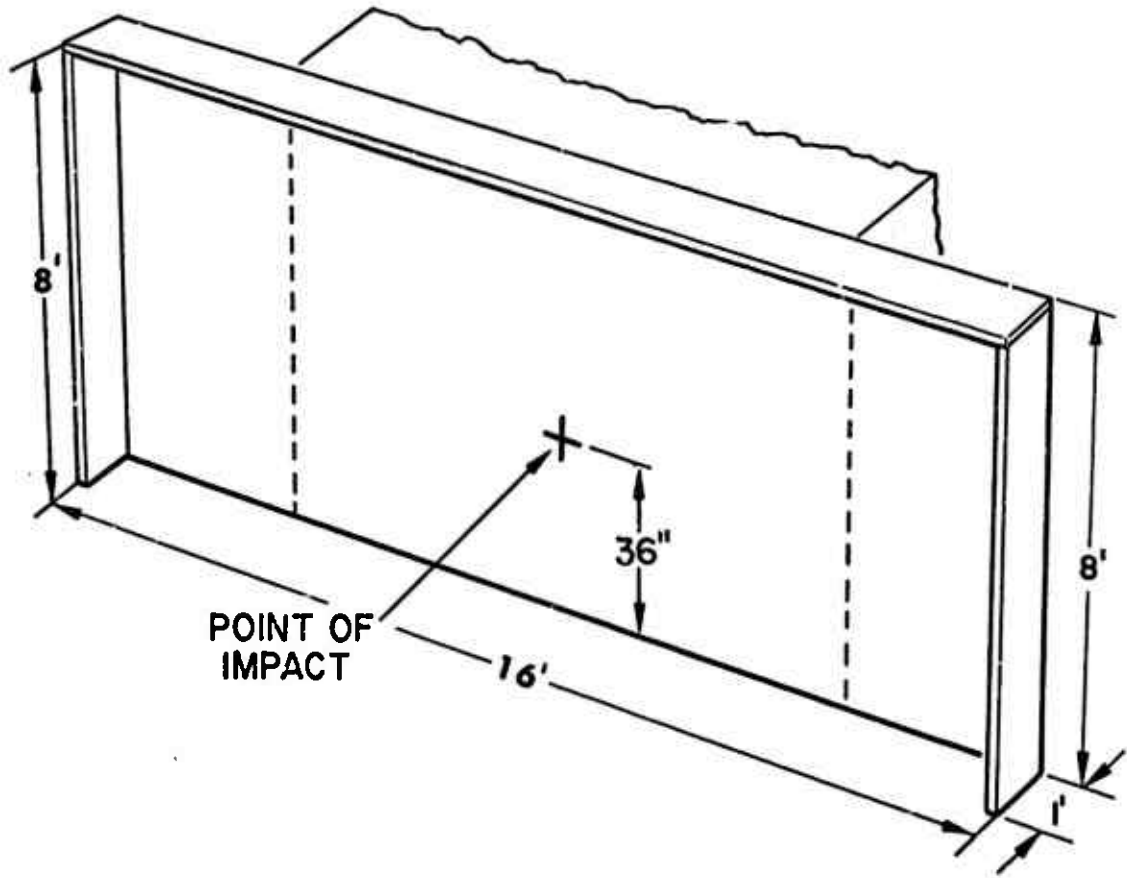


Fig. 5. Flat-Wall Target.



Fig. 6. Flat-Wall Target.

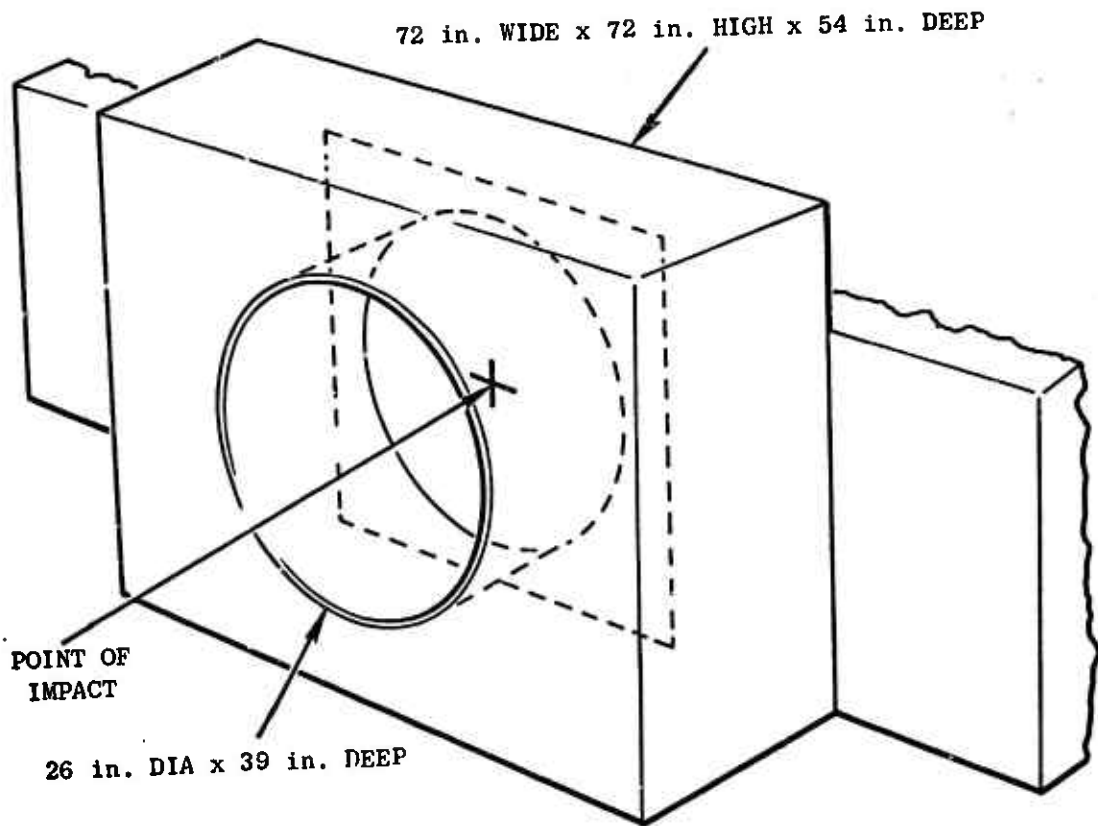


Fig. 7. Deep-Hole Target

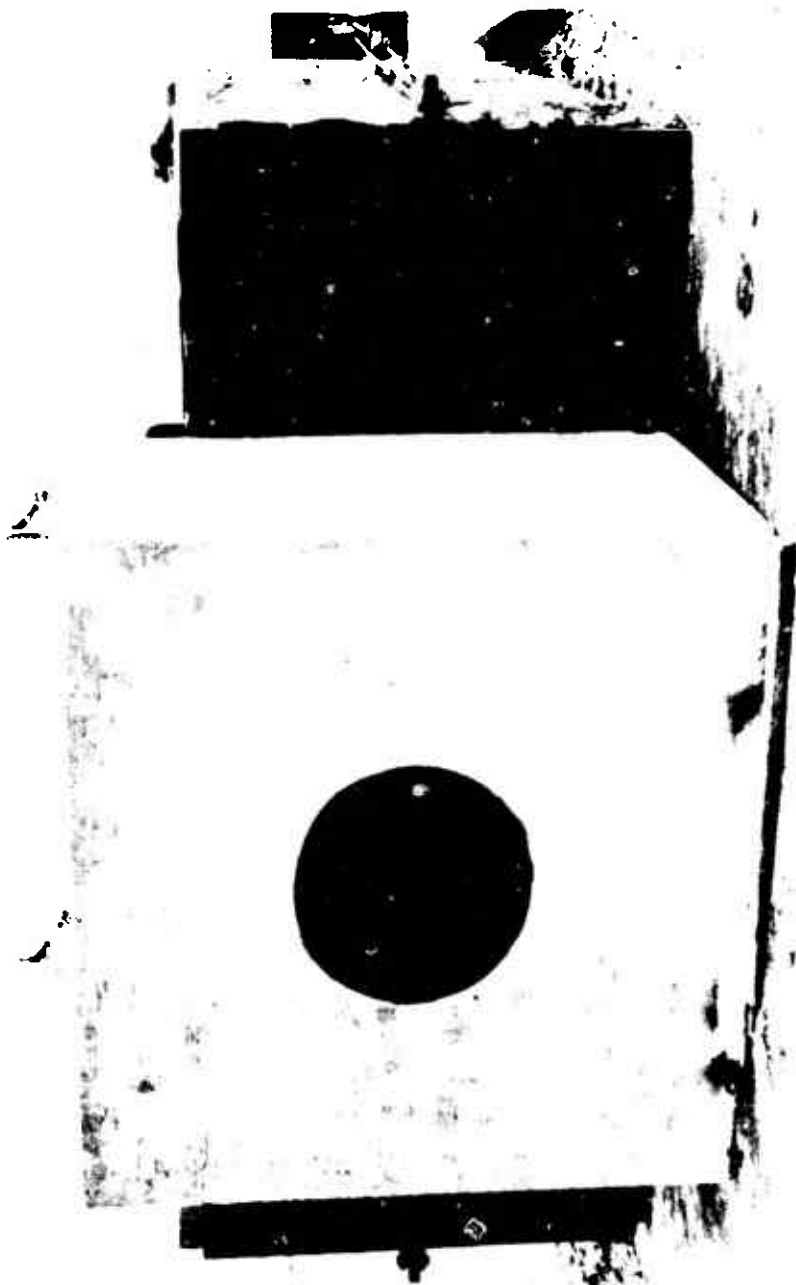


FIG. 8. Deep-Hole Target.

INSTRUMENTATION SYSTEM

The instrumentation layout used for the high-velocity-impact test series is shown in Fig. 9. The blast instrumentation system consisted of nine transducers positioned along three legs, 30, 90, and 180 deg from the track, and at nominal distances of 13, 23, 38 and 67 ft from the target. The transducers were natural quartz piezoelectric and were used with a charge-amplifier preamp.* The transducers were small, approximately 1/4 in. in diameter, with a 1/8-in. sensitive area. They were enclosed in a stainless steel housing, had a flush-mounted stainless steel diaphragm, and were mounted side-on to the blast wave in elevated gauge mounts (see Fig. 10).

TEST RESULTS

A summary of the test conditions for the hybrid high-velocity-impact test series is presented in Table 1. It will be noted that in addition to the three high-velocity-impact tests, two high-explosive functional tests and two high-explosive instrument calibration tests were conducted. The functional tests used 8-lb rectangular TNT blocks and the calibration tests used 18-lb spherical pentolite charges.

The individual peak overpressure and positive-phase-impulse data from the two 18-lb calibration tests are shown in Table 2** and are plotted as a function of scaled distance in Figs. 11 and 12. Included in these figures are curves representing the basic reference data obtained from approximately 12 flat-wall-

* Kistler Instruments Corporation transducer system 701A/566.

** These data have not been corrected for the difference in ambient pressure between sea level (14.7 psi) and that existing at the test site (approximately 13.7 psi). The correction is small and unnecessary for later yield computations because it is common to both the calibration and impact test data.

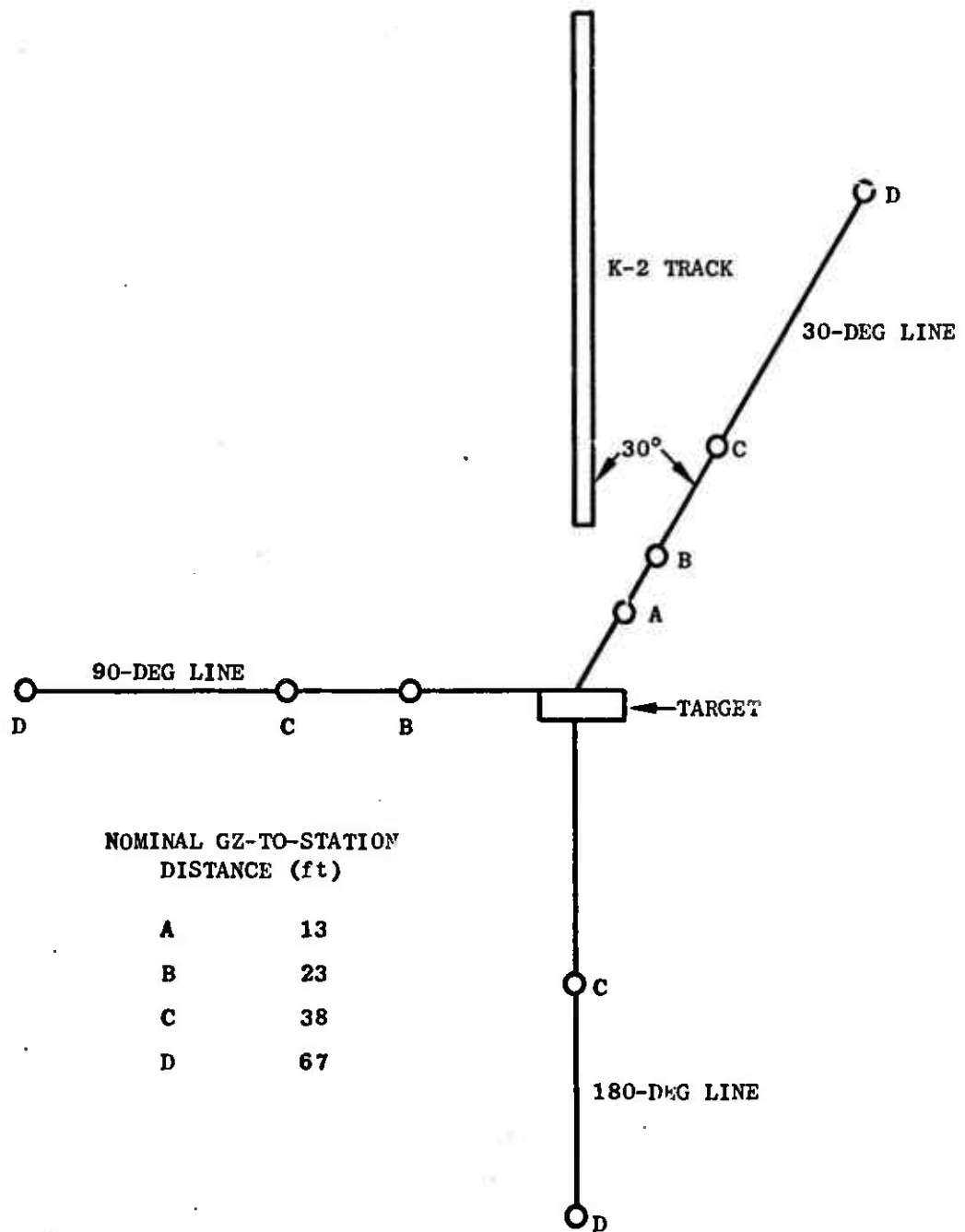


Fig. 9. Test Site and Instrumentation Layout for High-Velocity Hybrid Impact Tests.



Fig. 10. Typical Gauge Mount.

Table 1

SUMMARY OF TESTS FOR N_2O_4 /PBAN HIGH-VELOCITY-IMPACT-TEST SERIES

TEST NUMBER	WEIGHT (lb)	TYPE	IMPACT VELOCITY (fps)	TARGET CONFIGURATION
01	8	TNT*	-	Flat Wall
02	18	Pentolite**	-	Flat Wall
03	200	N_2O_4 /PBAN	691.8	Deep Hole
04	200	N_2O_4 /PBAN	591.7	Flat Wall
05	200	N_2O_4 /PBAN	586.8	Deep Hole
06	8	TNT*	-	Deep Hole
07	18	Pentolite**	-	Deep Hole

* Functional Check

** Instrument Calibration Test

Table 2
 PEAK OVERPRESSURE AND POSITIVE-PHASE-IMPULSE DATA FROM
 HIGH-EXLOSIVE CALIBRATION TESTS 2 AND 7

TARGET GEOMETRY	TEST NO.	GAUGE LINE PARAMETER	NOMINAL DISTANCE (ft)											
			13	23			38			67				
Flat Wall	2	Pressure (psi)	56	19	14	6.7	5.5	4.9	2.4	1.8	2.2	2.2	2.2	
		Impulse (psi-msec)	54	34	21	18	13	13	9.4	7.9	7.5	7.5	7.5	
		True Dist (ft)	13.3	22.8	23.3	38.2	38.2	38.8	67.2	67.4	68.8	68.8	68.8	68.8
Deep Hole	7	Pressure (psi)	52	20	5.4	8.6	3.6	3.7	2.8	0.8	1.1	1.1	1.1	
		Impulse (psi-msec)	55	37	12	24	9.9	6.6	11	6.7	4.5	4.5	4.5	
		True Dist (ft)	13.1	22.7	23.3	38.0	38.2	39.0	67.0	67.4	69.0	69.0	69.0	

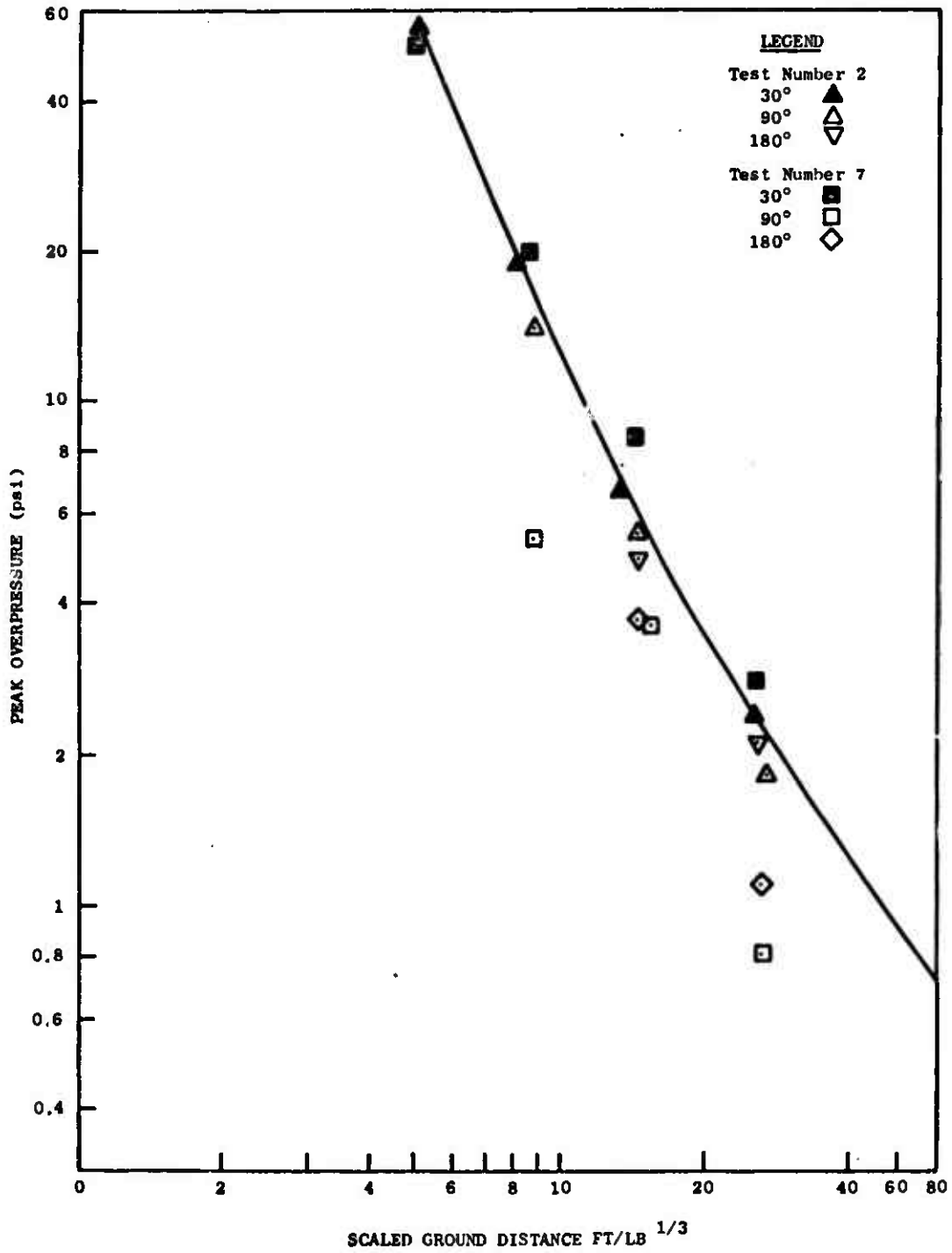


Fig. 11. Peak Overpressure vs Scaled Ground Distance for High Explosive Calibration Tests

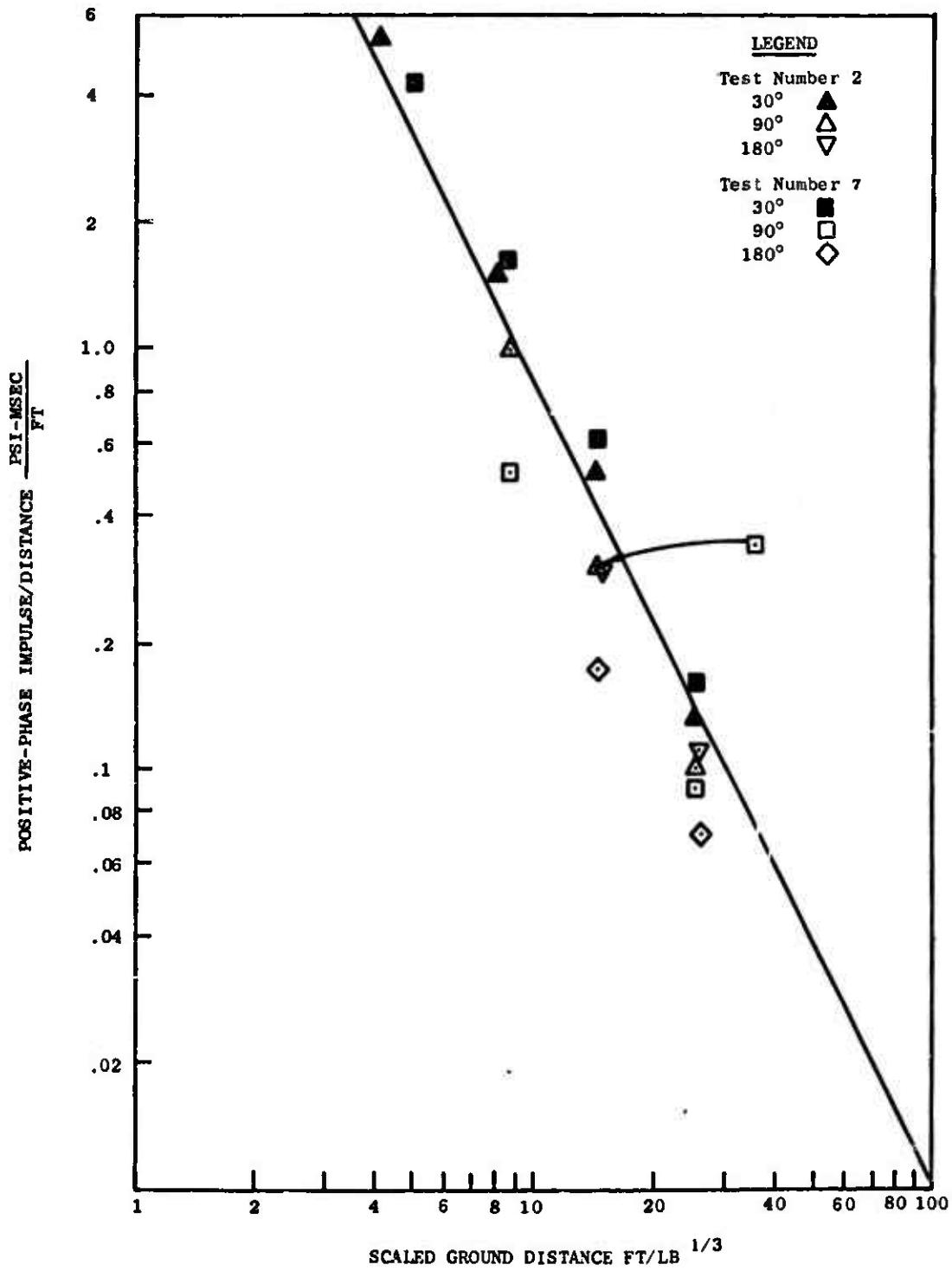


Fig. 12. Positive Phase Impulse vs Scaled Ground Distance for High Explosive Calibration Tests

target calibration tests using 18-, 105-, and 216-lb spherical charges, which have been conducted at this test site during the past 2 years. Note the excellent agreement between the data from the recent flat-wall calibration test (Test No. 2) and the basic reference curves. Also note the strong asymmetries indicated by the data from the one deep-hole calibration test (Test No. 7).

The peak overpressure and positive-phase-impulse data for the three N_2O_4 /PBAN impact tests are presented in Table 3. The yield values computed from the peak overpressure and positive-phase-impulse data (using the basic reference curves in Figs. 11 and 12, and multiplying by a factor of 1.18 to correct for the difference between pentolite and TNT) are given in Table 4.

The data in Table 4 indicates that large shock wave asymmetries are present, even at the outer gauge stations. This is particularly evident for the deep-hole-target tests. The persistence of these blast asymmetries over the entire measuring range tends to complicate the selection of appropriate terminal yield values for these tests since the test geometry is not completely similar to the full-scale case of concern. It will be recalled that these tests were intended to simulate nose-on impact of a vehicle at high velocity onto the ground surface. The flat-wall target was selected to simulate a rigid ground surface, in which no impact cratering would occur, while the deep-hole target simulated a soft ground surface, in which significant impact cratering would occur.

In the full-scale case of concern, it would be anticipated that blast pressure would be radially symmetrical about the point of impact along the ground surface and that blast asymmetry, if it existed, would occur in a vertical plane, with the pressure directly above the impact point being highest. Such asymmetries are not of much concern since pressure along the ground surface would be of most importance in the full-scale case.

In the test geometry, the tankage was accelerated along the ground surface on a sled track and allowed to impact on a massive vertical target since this was the only practical way to obtain the desired high velocities and the required control on the impact point.

Table 3
 PEAK OVERPRESSURE AND POSITIVE-PHASE-IMPULSE DATA FROM N₀₄/PBAN HIGH VELOCITY IMPACT TESTS

TARGET GEOMETRY	TEST NO.	GAUGE LINE (deg) PARAMETER	NOMINAL DISTANCE (ft)						
			13	23		38		67	
Flat Wall	4	Pressure (psi)	3.1	1.3	0.8	0.8	0.4	0.5	0.3
		Impulse (psi-msec)	4.0	4.0	1.7	1.7	1.2	1.5	0.4
		True Distance (ft)	14.28	23.38	23.27	39.18	38.17	63.21	67.42
Deep Hole	3	Pressure (psi)	13	7.1	0.8	3.2	11	1.4	0.8
		Impulse (psi-msec)	23	25	2.6	1.7	6.4	7.8	4.6
		True Distance (ft)	13.11	22.66	23.27	38.01	38.17	67.04	67.42
Deep Hole	5	Pressure (psi)	7	4.2	1.1	1.7	5.6	0.7	3.7
		Impulse (psi-msec)	10	11	2.2	0.5	1.7	0.4	1.1
		True Distance (ft)	13.11	22.66	23.27	38.01	38.17	67.04	67.42

Table 4
EXPLOSIVE YIELDS FROM N₂O₄/PBAN HIGH VELOCITY IMPACT TESTS

TARGET GEOMETRY	TEST NO.	GAUGE LINE (deg) YIELD %	NOMINAL DISTANCE (ft)						
			13	23		38		67	
Flat Wall	4	Pressure Yield	0.2	0.2	0.04	0.2	0.03	0.4	0.08
		Impulse Yield	0.3	0.7	0.2	0.3	0.2	0.5	0.07
	3	Pressure Yield	1.3	2.7	0.04	3.3	0.9	3.5	1.2
		Impulse Yield	4.4	11.0	0.3	6.6	2.7	7.3	3.6
Deep Hole	5	Pressure Yield	0.4	1.2	0.1	1.0	0.06	0.7	0.1
		Impulse Yield	1.2	2.8	0.2	2.1	0.4	2.4	0.4

The important differences between the real and test geometries can be understood by visualizing that the test geometry is created by rotating the line of flight of the test tankage and a section of the ground surface the size of the target through 90 deg, as shown in the following sketch (Fig. 13).

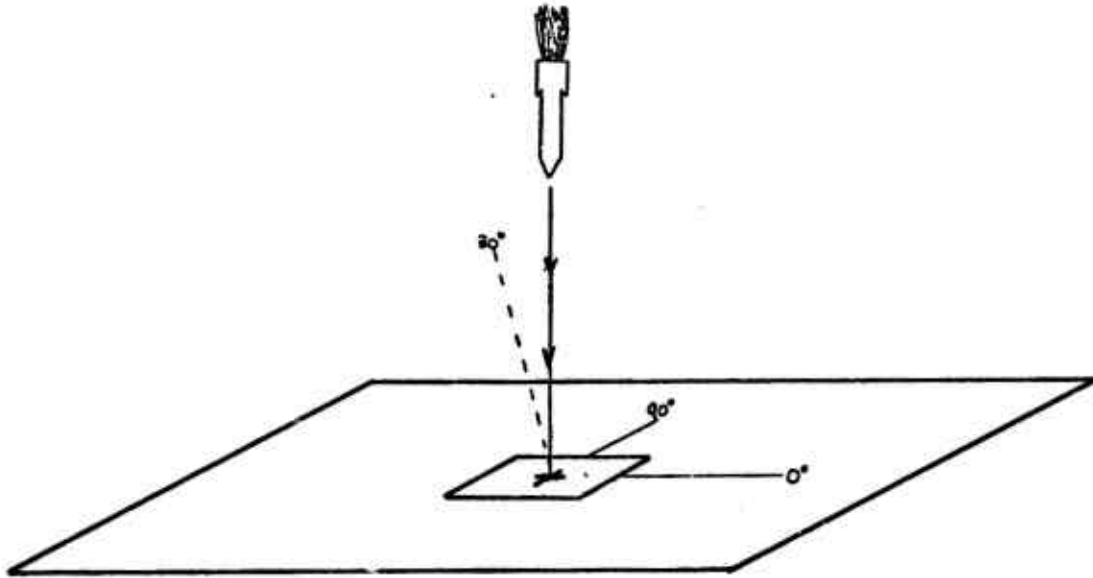
From this sketch it appears that the pressures along the 90-deg gauge line in the test geometry case would most nearly correspond to the pressures along the ground surface in the real geometry. The pressures along the 30-deg line in the test geometry tend to correspond with those at 30 deg from the vertical in the real geometry and thus would be higher than the ground-surface value. The pressures along the 130-deg gauge line in the test geometry would clearly tend to be lower than the ground-surface pressure in the real geometry.

These considerations suggest several possible methods for estimating appropriate terminal yields. For example:

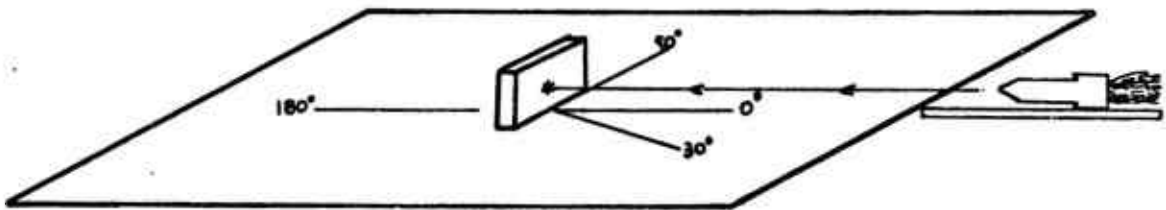
1. Use value for 90-deg gauge line.
2. Use average of maximum and minimum values where the minimum value corresponds to that for the 180-deg gauge line and the maximum value to that along the line of flight (this value would have to be obtained by extrapolation).
3. Use a combination of 1 and 2.

Preliminary comparison of yields computed by methods 1 and 2 indicates that the average of the maximum and minimum value was generally larger than the value for the 90-deg gauge line; however, the differences were small.

In an attempt to weigh all experimental data in an equal fashion, the method finally selected involved averaging the terminal yield in the 0-, 90-, and 180-deg directions with the 0-deg value obtained by extrapolation. (Plots showing the extrapolated values are given in Fig. 14. Since the yields of these tests were very low, no measurable results were obtained from the 180-deg-leg instrumentation. Based on the gain setting used for this instrumentation, it has been estimated that the yield must have been less than 0.03%, and this is the value that was used in the computation. The yield values computed in this manner are presented in Table 5.

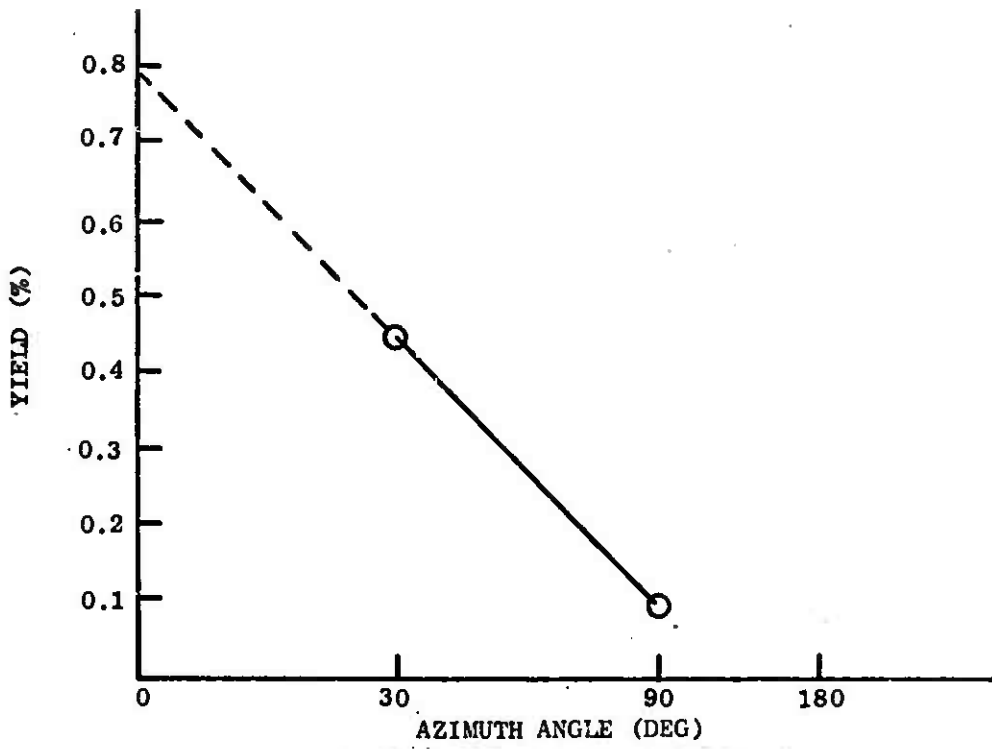


Full-Scale Geometry

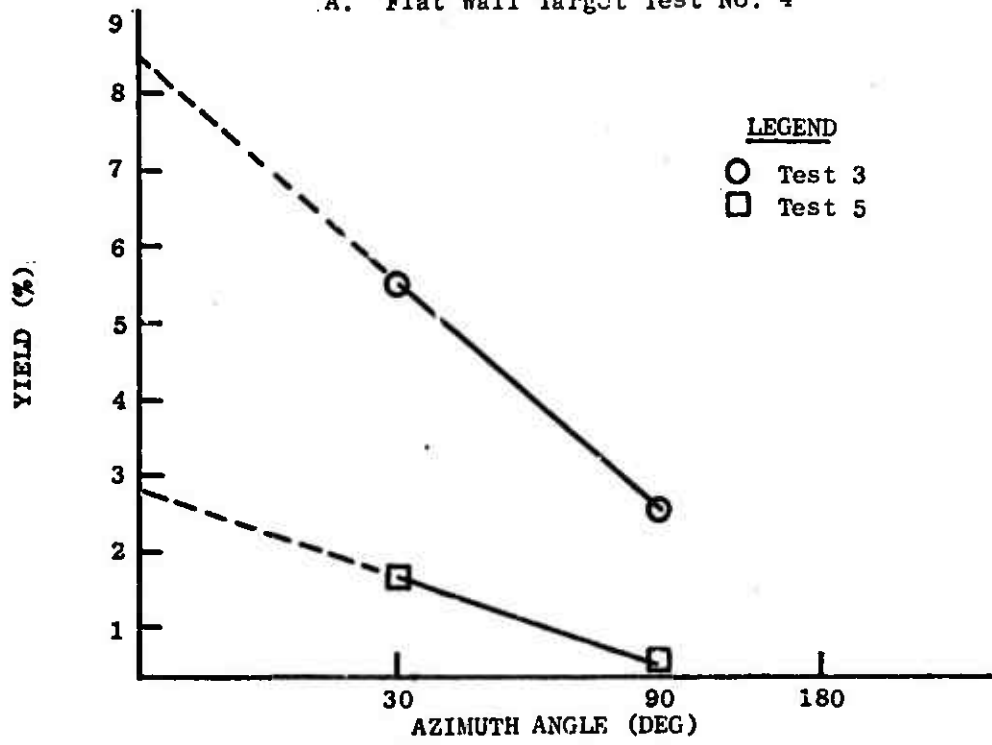


Test Geometry

Fig. 13. Sketch Indicating Differences Between Full-Scale and Test Geometry.



A. Flat Wall Target Test No. 4



B. Deep Hole Target Test Numbers 3 and 5

Fig. 14. Plots Showing Method of Extrapolation to Obtain 0 Deg Yield Values (see text).

Table 5

TERMINAL YIELDS FROM N_2O_4 /PBAN-HIGH-VELOCITY-IMPACT TESTS

TARGET GEOMETRY	TEST NO.	TERMINAL YIELD (%)
Flat Wall	4	0.4
Deep Hole	3	4.3
	5	1.4

Section 4

 N_2O_4 /PBAN EXPLOSIVE-DONOR AND DROP-TEST SERIES

The explosive-donor portion of the series consisted of three tests in which 30-lb cylindrical Composition B charges (donors) were detonated immediately above cylindrical tanks containing the hybrid propellant combination. Two tests were conducted with the solid (PBAN) in the top compartment (adjacent to the charge) and the liquid (N_2O_4) in the bottom compartment and one test in which the propellants were reversed, i.e., the liquid was on top and the solid on the bottom.

The drop-test portion of the series consisted of two tests in which cylindrical tanks of the hybrid propellant combination were dropped from a 101-ft drop tower and allowed to impact on the test pad. In the first drop test, nose-on impact propellant orientation was used, i.e., the N_2O_4 was placed in the bottom compartment and impacted the ground first. In the second test the propellants were reversed, and the PBAN was allowed to impact the ground surface first.

A simulated ignition source in the form of a sealed container containing 0.5 lb of hydrazine (N_2H_4) was included in each of the explosive-donor and drop tests.

TANKAGE FOR THE EXPLOSIVE-DONOR TEST SERIES

A sketch of the test tank designed and fabricated for the explosive donor test series is shown in Fig. 15. These tanks were cylindrical in shape, 12.8 in. in diameter, and 42.25 in. long. The cylinder walls were 0.060-in. aluminum and the diaphragms separating the propellants were 0.003 in. aluminum foil. The tanks contained approximately 120 lb of N_2O_4 and 80 lb of PBAN. The PBAN was cast in place in a "wagon wheel" pattern using a removable wooden mold. A photograph of an explosive-donor tank with the explosive donor in place is shown in Fig. 16.

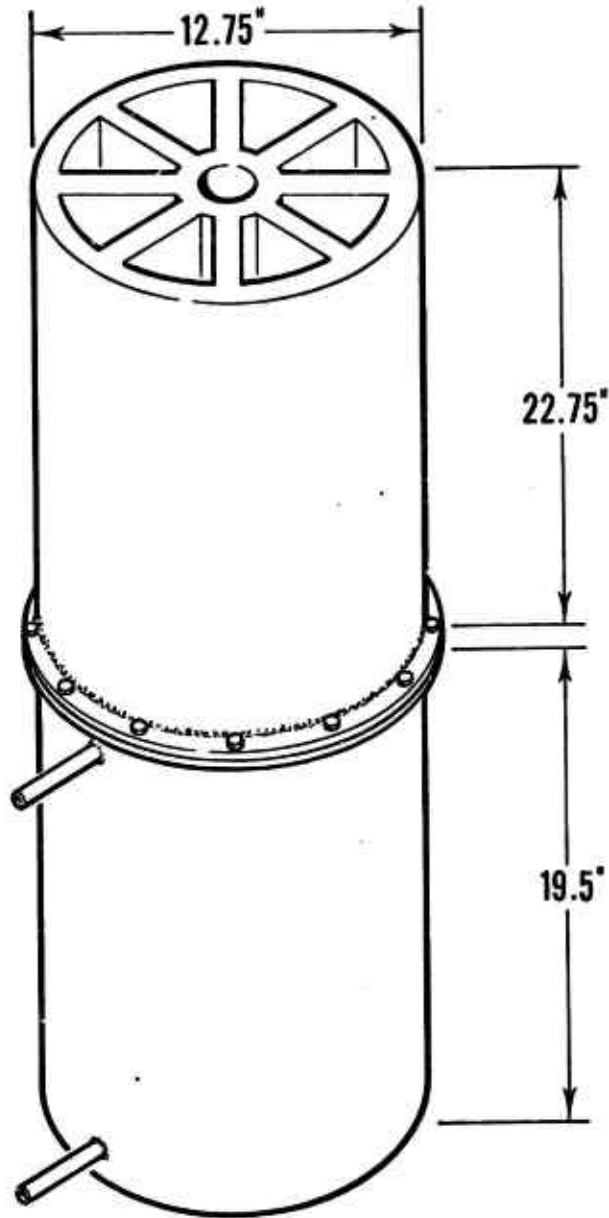


Fig. 15. N_2O_4 /PRAN Explosive-Donor Tank

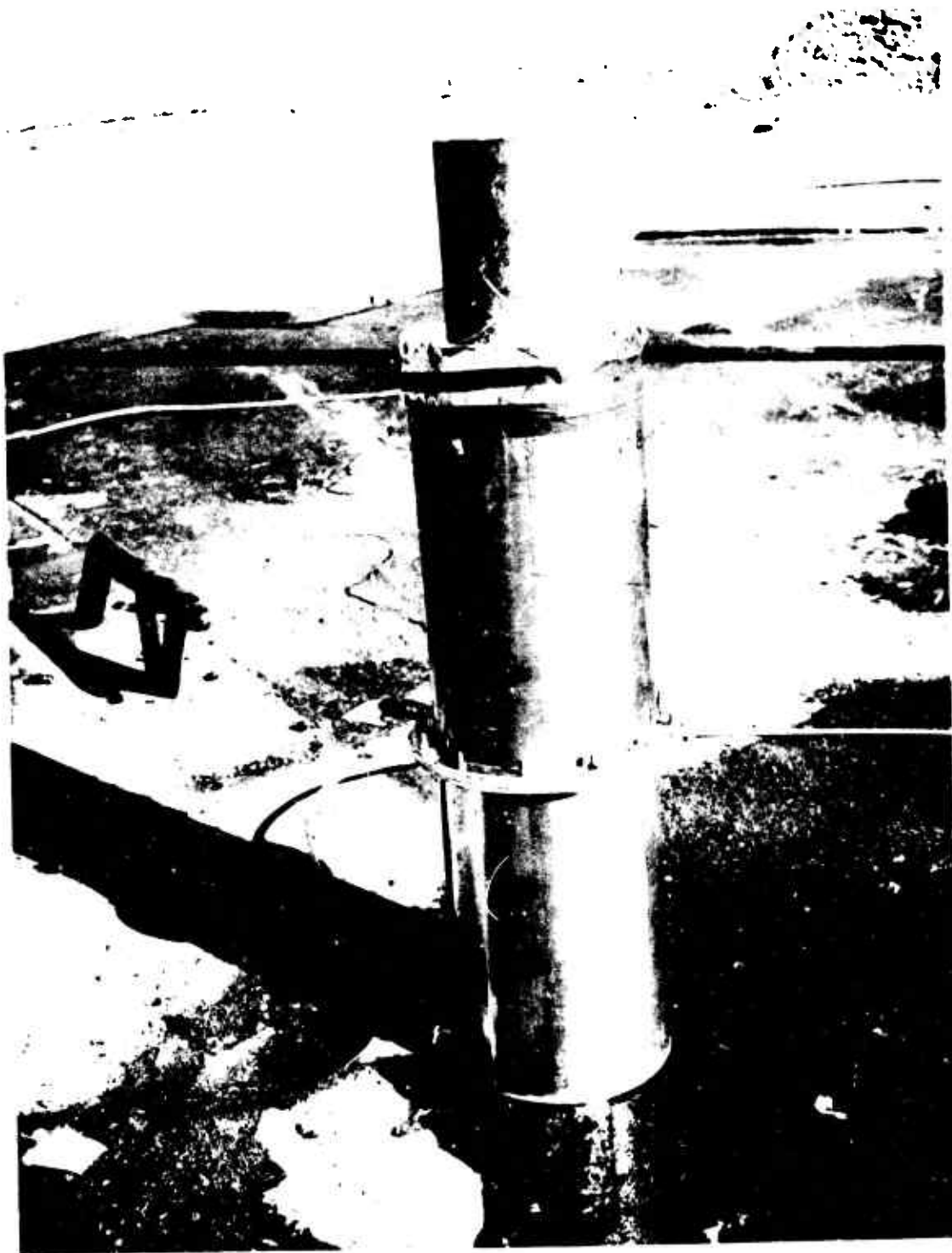


Fig. 16. N_2O_4 /PBAN Explosive Donor Tank with 30-lb Donor in Place.

DROP TEST TANKS

A sketch of the test tank designed for the drop-test series is shown in Fig. 17. This tank is similar to the explosive-donor tanks, being cylindrical in shape, 12.75 in. in diameter, 42.25 in. long, and having 0.060-in. aluminum walls. The major differences, however, are a much stronger diaphragm, which was fabricated of two sheets of 0.003-in. aluminum foil and the roller bearing "skates" used to fasten the tank to the drop tower track.

The drop tower used in this test series was 101 ft high and was specifically designed for propellant-hazard testing. A sketch of this tower is shown in Fig. 18. The lower 30 ft of this tower was composed of tripod legs fabricated from 6-in. double-extra-strong pipes. The remaining 71 ft of the tower was a high-strength version of a standard radio antenna tower, with the vertical members of this section fabricated from seamless mechanical tubing. Installed on this tower are work platforms, instrumentation conduits, propellant fueling lines, and a T-shaped track affixed to one side of the tower to guide the test tanks. Dropping the tanks was accomplished by an explosive cable-cutting device detonated after the oxidizer was remotely loaded at the top of the tower.

INSTRUMENTATION SYSTEM

The blast instrumentation system used for this test series consisted of 23 pressure gauges distributed along three radial lines, 120 deg from each other, and spaced over a ground distance of approximately 4 to 200 ft. The gauges used were the same natural quartz piezoelectric pressure transducers described in the high-velocity-impact instrumentation section.

In addition to the blast instrumentation, a thermal instrumentation system was used in this series of tests. The measurements made included: radiometer measurements external to the fireball, radiometer measurements within the fireball, and surface-temperature measurements of stainless steel and copper slabs located within the fireball. A more complete description of the thermal instrumentation is included with a presentation of thermal data later in this section.

A summary of the blast and thermal instrumentation is presented in Table 6 and Fig. 19.

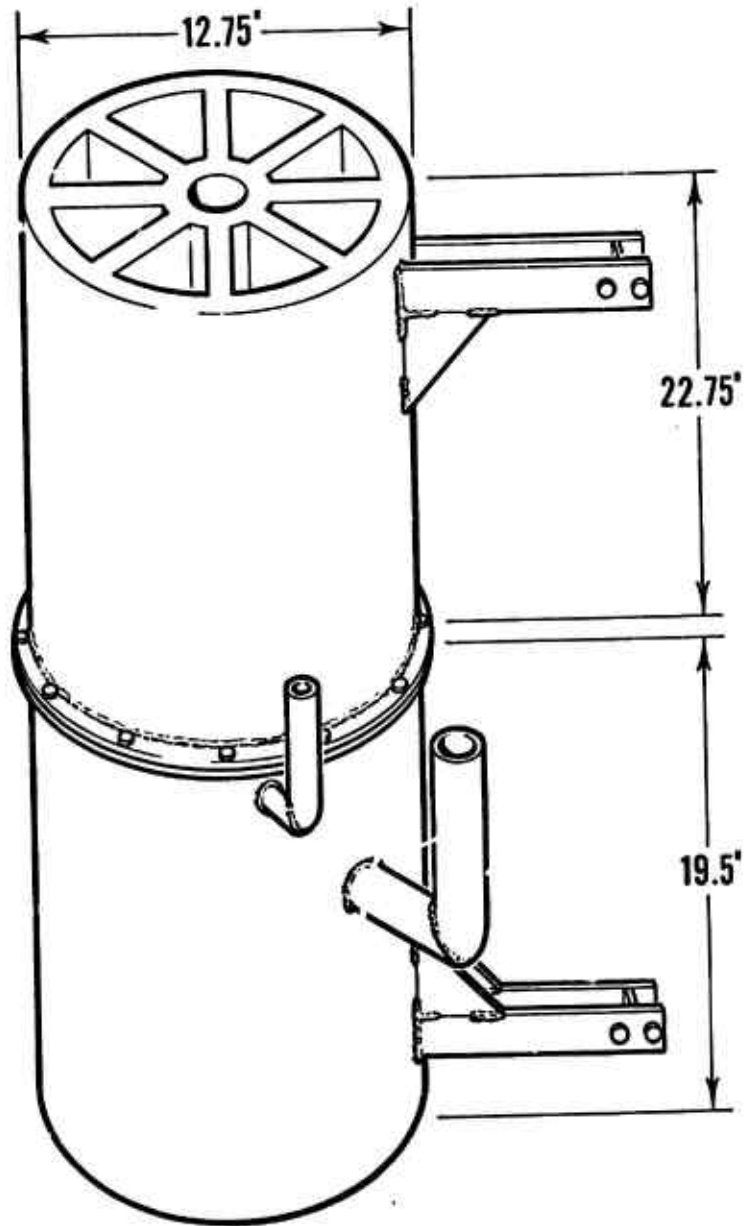


Fig. 17. Sketch of N_2O_4 /PBAN Drop Tank

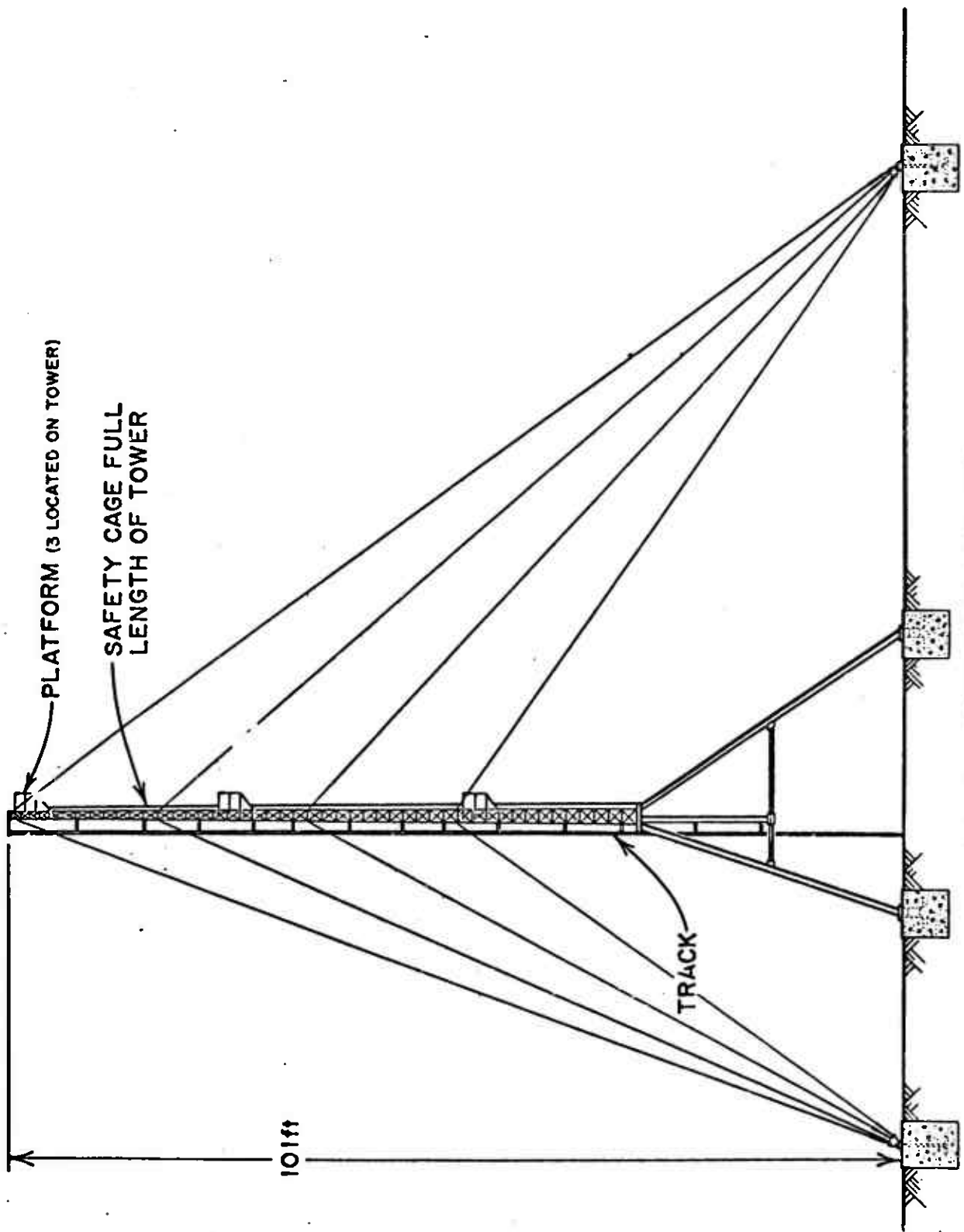


Fig. 18. Sketch of the Drop Tower

Table 6
INSTRUMENTATION LAYOUT AT AFRPL

NO.	GAUGE LINE	NOMINAL DISTANCE (ft)	PRESSURE	
			P _s *	P _o **
I	A B C	2.8		X
II	A B C	4.5	X	X
III	A B C	7.5	X X	X X X
IV	A B C	13	X	X X X
V	A B C	23		X X X
VI	A B C	38		X X X
VII	A B C	67		X X X
VIII	A B C	117		X X X
IX	A B C	200		X X X

* P_s = Head-on-oriented stagnation pressure sensor

** P_o = Side-on-oriented overpressure sensor

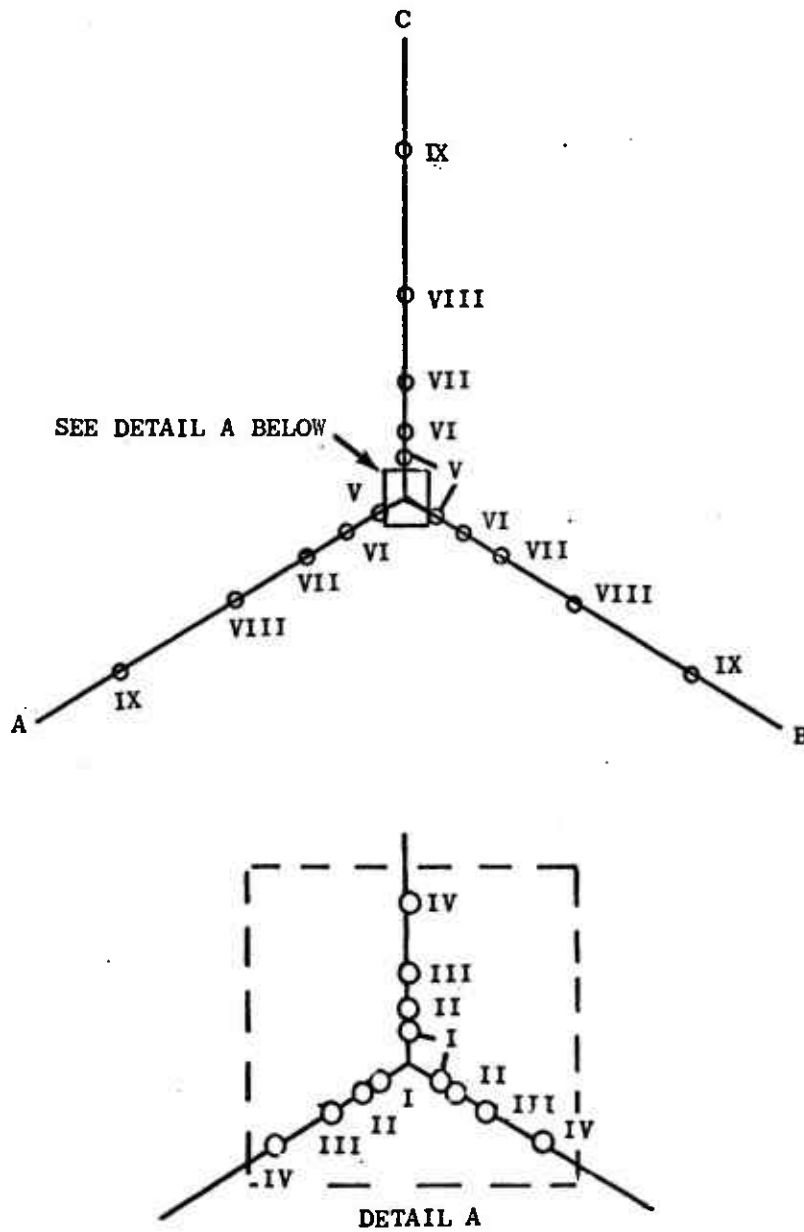


Fig. 19. Instrumentation Layout

The basic sensor mount designs used in the blast and thermal instrumentation systems for this test series are shown in Figs. 20, 21, and 22.

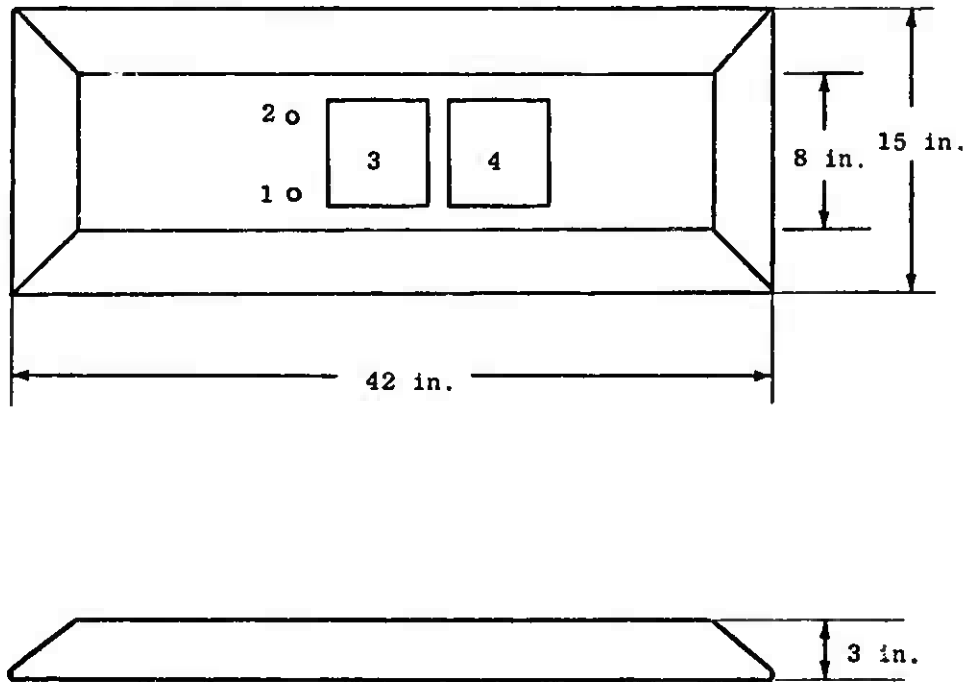
The type A mounts (Fig. 20) are fabricated from 3-in.-thick solid steel and are used in the close-in environment. The configuration shown, located 7.5 ft from ground zero, contains a side-on overpressure sensor, stagnation pressure sensor, and two surface-temperature Delta-Couple plates.

The type B mount (Fig. 21) is located 23 ft from ground zero and is fabricated from 3-in.-diameter, heavy-wall stainless steel tubing. The front nose of this mount is removable to allow use of either the pointed nose containing the stagnation sensor or a blunt protective nose. A side-on-overpressure sensor is located on top of the mount, as noted in the figure.

The type C mount (Fig. 22) combines the type B with a 12-in.-high raised pedestal. The purpose of this pedestal at the stations within the fireball is to contain the surface-temperature thermal instrumentation (indicated by dotted lines in Fig. 22). At the stations external to the fireball, the additional height of the raised pedestal helps to prevent ground surface irregularities and the dust created by the explosions from influencing the overpressure readings. These mounts are used at distances from 37 to 200 ft from ground zero.

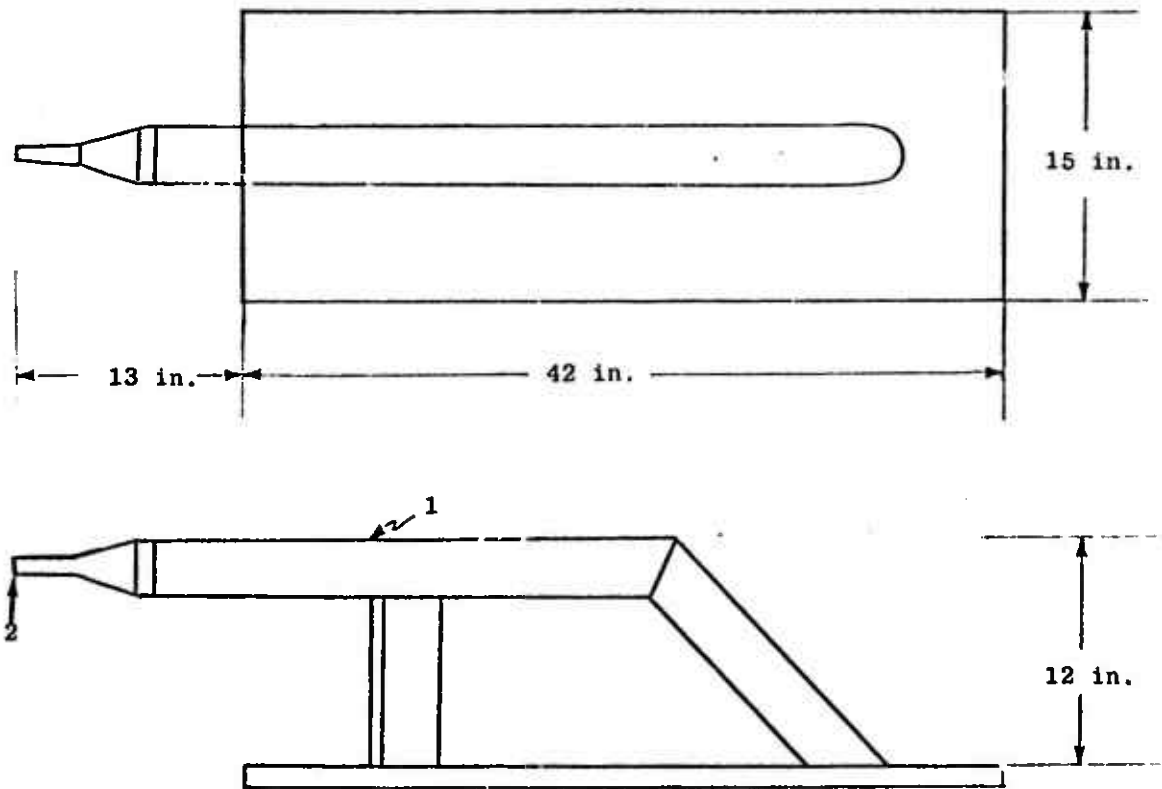
TEST RESULTS

A summary of the test conditions for the explosive-donor and drop-test series is presented in Table 7. For the explosive-donor case it will be noted that there were three propellant tests and one inert test (i.e., both propellants were replaced by water). This latter test was conducted because it was suspected that the contribution to peak overpressure and impulse by this 30-lb donor charge might be large compared to the propellant. If this occurred, separation of the yield (effective charge weight) of the propellant from that of the donor would be extremely uncertain unless the results from the donor charge itself were known quite well.



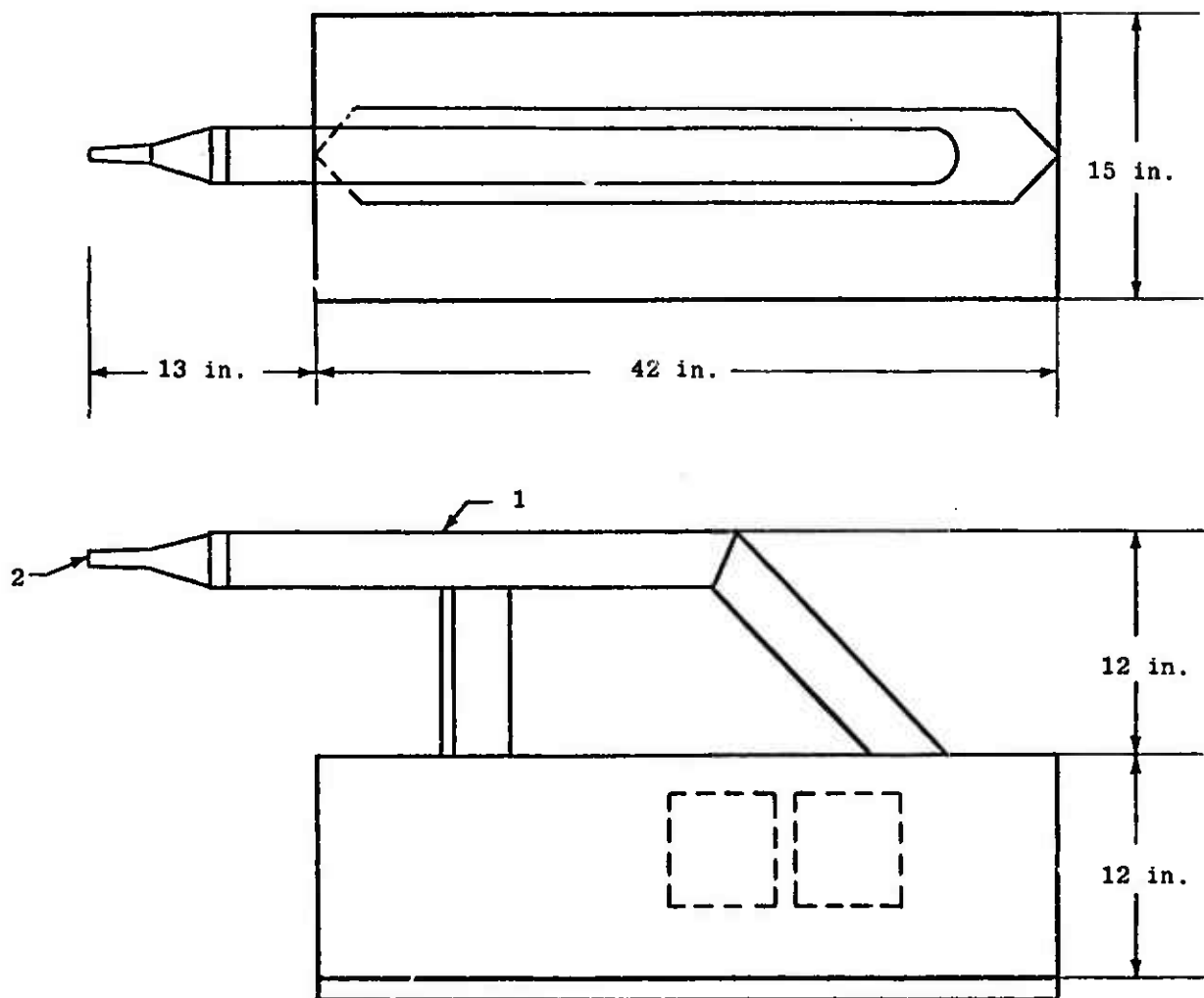
1. Side-on overpressure gauge
2. Stagnation gauge
3. T_c Copper Delta-Couple plate
4. T_s Stainless steel Delta-Couple plate

Fig. 20. Type A Sensor Mount



- 1. P_o Side-on overpressure gauge
- 2. P_s Stagnation gauge

Fig. 21. Type B Sensor Mount



1. P_o Side-on overpressure gauge
2. P_s Stagnation gauge

Fig. 22. Type C Sensor Mount

Table 7

SUMMARY OF TEST CONDITIONS FOR N_2O_4 /PBAN
EXPLOSIVE-DONOR AND DROP-TEST SERIES

EXPLOSIVE-DONOR TEST SERIES

TEST NUMBER	PROPELLANT WEIGHT (LB)	PROPELLANT ORIENTATION	DONOR
241	200	Inert test-tank filled with water	30-lb cylinder
243	200	PBAN on top- N_2O_4 on bottom	30-lb cylinder
244	200	N_2O_4 on top-PBAN on bottom	30-lb cylinder
259	200	PBAN on top- N_2O_4 on bottom	30-lb cylinder

DROP-TEST SERIES

TEST NUMBER	PROPELLANT WEIGHT (LB)	IMPACT VELOCITY FT/SEC	PROPELLANT ORIENTATION
260	200	~75	PBAN on top- N_2O_4 on bottom
261	200	~75	N_2O_4 on top-PBAN on bottom

The peak overpressure and impulse data obtained from the explosive-donor tests are presented in Table 8. Terminal yield values have been computed for each of these tests and are presented in Table 9. The yield values were determined by computing the mean of the yield, both pressure and impulse, obtained at each of the outer gauge stations (67, 117 and 200) and subtracting the yield values of the test with water from those of the tests with the propellants.

No measurable deflections were obtained on the pressure records from the drop tests. In the first test, in which the N_2O_4 impacted the ground first, no evidence of any ignition or fire could be seen. The solid (PBAN) tank was only slightly damaged, and the N_2H_4 cylinder was recovered intact. In the second test, in which the solid (PBAN) impacted first, the N_2H_4 cylinder was crushed and a fire started several seconds after impact. No sound from this test was detectable at the blockhouse, so it is doubtful that any explosion occurred.

Since no actual pressure data were obtained, only estimates of the upper bounds on the yield values from these tests can be made. From the instrumentation gain settings used for these tests, it has been estimated that a yield of 0.005% would have given a detectable trace deflection.

THERMAL MEASUREMENTS

Within the fireball, measurements were made of the surface temperature of copper and stainless steel slabs and of radiant intensity (the radiant energy per unit area per unit time), while at locations outside the fireball radiant intensity alone was measured.

The intra-fireball radiometers have essentially a 180-deg field-of-view, i.e., receive energy over a half-space, so that their output is a representation of the radiant intensity incident on a planar opaque surface immersed in the fireball.* The field-of-view of the external radiometers includes the entire fireball. The radiometer response time, i.e., time to reach 90% deflection, is estimated to be 15 msec.

* As noted below, this is true only after corrections to the raw data are made.

Table 8

PEAK OVERPRESSURE AND POSITIVE PHASE-IMPULSE DATA FROM N_2O_4 /PBAN
EXPLOSIVE DONOR TESTS

TEST NO.	TEST TYPE	PARAMETER MEASURED	GAUGE LINE	NOMINAL DISTANCE (ft)				
				23	37	67	117	200
241	Charge and Water Only	Pressure	1	-	9.1	3.1	1.5	0.8
			2	28.4	8.2	2.9	1.5	0.7
			3	28.0	-	2.9	-	1.4
			Average	28.2	8.7	3.0	1.5	1.0
		Impulse	1	-	-	14.0	8.6	-
			2	31.7	22.4	13.5	8.0	4.9
3	31.1		-	14.5	8.4	4.5		
Average	31.4		22.4	14.0	8.3	4.7		
243	Charge and Propellant 1	Pressure	1	42.8	11.3	3.8	1.7	-
			2	35.7	10.5	3.1	1.8	0.9
			3	34.9	10.3	-	1.7	0.8
			Average	37.8	10.7	3.5	1.7	.9
		Impulse	1	39.5	30.9	19.0	12.0	7.1
			2	38.3	34.4	18.7	11.8	6.8
3	42.4		31.7	19.7	10.9	6.4		
Average	40.1		32.3	19.1	11.6	6.8		
244	Charge and Propellant 2	Pressure	1	-	10.8	3.5	1.7	-
			2	33.8	9.4	2.9	1.5	0.8
			3	30.6	9.5	-	1.5	0.8
			Average	32.2	9.9	3.2	1.6	0.8
		Impulse	1	-	26.1	16.9	10.5	5.9
			2	33.4	26.7	15.4	8.9	5.8
3	35.4		28.9	16.9	9.8	5.3		
Average	34.4		27.2	16.4	9.7	5.7		
259	Charge and Propellant 1	Pressure	1	-	-	-	-	0.8
			2	33.6	8.3	-	1.9	0.9
			3	30.0	9.8	-	-	0.9
			Average	31.8	9.1	-	1.9	0.9
		Impulse	1	29.9	50	-	-	7.3
			2	51.2	32.6	-	12.2	6.6
3	41.7		32.8	-	-	6.6		
Average	40.9		38.5	-	12.2	7.5		

1. PBAN on top N_2O_4 on Bottom.
2. N_2O_4 on top PBAN on Bottom.

Table 9
TERMINAL YIELDS FROM N_2O_4 /PBAN
EXPLOSIVE DONOR TESTS

TEST NUMBER	TERMINAL YIELD %
243	8.7
259	12.6
244	4.7

The slab surface temperature measurements were obtained via thermocouple junctions at depths of 0.002 and 0.005 in. below the exposed surface of the slab for the stainless steel (309) and copper, respectively. The slab thickness was 1 in., so that over the duration of the heating pulse, the slabs represent semi-infinite slabs, i.e., the temperature of the exposed surface is not influenced by the discontinuity presented by the back surface.

Three external radiometers were used, two located at 67 and 117 ft from ground zero along Gauge Line A, with the third at 67 ft along Gauge Line B, making an angle of 120 deg with the first (see Fig. 19). The internal radiometer was 10 ft from ground zero along Gauge Line A, mounted with its receiving surface flush with a horizontal steel plate at a height of 3.5 ft so that it "viewed" the half-space above.

Adjacent copper and stainless steel slabs were positioned at a ground distance of 7.5 and 13 ft along Gauge Line A and at 13 ft along Gauge Line B. Illustrations of the slab orientation and mounting are given in Fig. 18 for the slabs at 7.5 ft and in Fig. 20 for those at 13 ft.

As can be noted from Fig. 22, the exposed (and instrumented) surfaces of the slabs at the 13-ft distance were oriented side-on to the flow. Two adjacent stainless steel slabs, one with a thin, black absorbing layer on its exposed surface, were elevated 3.5 ft from the ground surface and 10 ft from ground zero along Gauge Line A. The exposed surface of the elevated slabs was parallel to the ground surface, similar to the slabs shown for the 7.5-ft station on Fig. 18. In addition, two adjacent stainless steel slabs, one of which was coated black, were located about 12 ft above the ground surface almost directly above ground zero. The exposed surface of these slabs was also oriented side-on to the flow. All of the above-mentioned slabs were mounted with their exposed surface flush with the mount, and except as noted above, the exposed surface was polished.

One further surface temperature measurement was made. A hemicylindrical block (4 in. diameter 12 inches long) was located at the 13-ft Gauge Line B station so that its curved surface was toward ground zero. A thermocouple was located at a depth of 0.005 in. beneath the curved surface at the stagnation point, that is, head-on to the flow.

Before considering the data, which are presented in Table 10, it is appropriate to briefly discuss the limitations of the thermal instrumentation system for this particular series of tests. Ordinarily the instrumentation system described above is used in conjunction with tests with various liquid propellant combinations, which for most combinations and test conditions, result in thermal instrumentation responses that are large compared to those that are considered here. By way of illustration, full-scale deflections are typically pre-set for 200-lb of propellants at about 150 and 75°C for the stainless steel and copper surface temperatures respectively, and 100 watts/cm² for the intra-fireball radiant intensity. Moreover, when a previously untested propellant combination is initially encountered, it is the policy to maintain these full-scale settings even though the response may be inordinately low with a correspondingly large uncertainty. Such a policy is maintained since (1), it is difficult to reliably predict the response from some previously untested propellants, (2), there tends to be a large test to test variation with the same propellant combination under similar test conditions, and (3), there is decreasing concern regarding accuracy as the thermal hazard or response decreases. Accordingly, since the response from these tests was comparatively low, the data at best provides, as will be numerically indicated below, a general magnitude. A complete quantitative description of uncertainties is considerably more involved than is thought to be practical under these circumstances (a detailed error analysis is given in URS 652-10).^{*} It appears more appropriate to give a quantitative notion of the uncertainties by listing estimates of the uncertainties of the peak or maximum value of each data trace. These are listed in column 7 of Table 10.

The data in Table 10, are presented in terms of characteristic magnitudes, which include their peak or maximum magnitudes, the time after ignition at which the peaks occur, and the approximate duration of the radiant intensity pulse. In addition, illustrations of the slab surface temperature-time and radiant intensity-time traces, taken primarily from Test 243, are presented in Fig. 23 through 25.

* C. Wilton, J. Mansfield, and A. B. Willoughby, Study of Liquid Propellant Blast Hazards, AF 04(611)-10739, URS 652-10, Dec. 1965.

Table 10
THERMAL DATA

TEST NO.	PARAMETER: TEMPERATURE OR RADIANT INTENSITY	STATION			MAXIMUM VALUE: TEMP (°C) RADIANT INTENSITY (WATT/CM²)	ESTIMATED UNCERTAINTY (%)	SLAB MATERIAL: STAINLESS STEEL (SS); COPPER (CU)	SLAB SURFACE: CLEAN (C); COATED BLACK (B)	TIME OF PULSE MAXIMUM (MSEC)	ESTIMATED DURATION (MSEC)
		GROUND DISTANCE (FT)	HEIGHT (FT)	GAUGE LINE						
241	Temperature	0	13	-	3.5	50	SS	B	-	-
		7.5	0	A	8	30	SS	C	30	-
		7.5	0	A	2	50	CU	C	20	-
		10	3.5	A	23	50	SS	B	10	-
		10	3.5	A	B	30	SS	C	10	-
	Radiant Intensity	13	0	A	2	50	SS	C	70	-
		13	0	B	-	-	SS	C	-	-
		13	0	B	-	-	CU	C	-	-
		13	0	B	5*	30	CU	C	50	-
		10	3.5	A	4	50	-	-	-	-
244	Temperature	67	0	A	0.30	50	-	-	-	-
		67	0	B	0.35	50	-	-	-	-
		117	0	A	0.15	30	-	-	-	-
		0	13	-	-	-	SS	B	-	-
		0	13	-	-	-	SS	C	-	-
	Radiant Intensity	7.5	0	A	8	30	SS	C	10	-
		7.5	0	A	1.8	50	CU	C	10	-
		10	3.5	A	31	30	SS	B	10	-
		10	3.5	A	10	50	SS	C	10	-
		13	0	A	8	30	SS	C	20	-
Radiant Intensity	13	0	A	1.2	50	CU	C	-	-	
	13	0	B	3	50	SS	C	-	-	
	13	0	B	0.8	50	CU	C	-	-	
	10	3.5	A	10	50	-	-	30	100	
	67	0	A	0.5	50	-	-	30	100	
									30	100
									30	100

Table 10 (Cont.)
THERMAL DATA

TEST NO.	PARAMETER: TEMPERATURE OR RADIANT INTENSITY	STATION			ESTIMATED UNCERTAINTY (%)	SLAB MATERIAL: STAINLESS STEEL (SS); COPPER (CU)	SLAB SURFACE: CLEAN (C); COATED (B)	TIME OF PULSE MAXIMUM (MSEC)	ESTIMATED DURATION (MSEC)
		GROUND DISTANCE (FT)	HEIGHT (FT)	GAUGE LINE					
243	Temperature	0	12	-	30	SS	B	150	-
		0	12	-	50	SS	C	-	-
		7.5	0	A	15	SS	C	300	-
		7.5	0	A	15	CU	C	300	-
		10	3.5	A	25	SS	B	100	-
		10	3.5	A	15	SS	C	100	-
	Radiant Intensity	13	0	A	25	SS	C	100	-
		13	0	A	50	CU	C	-	-
		13	0	B	15	SS	C	70	-
		13	0	B	25	CU	C	70	-
		13	0	B	15	CU	C	70	-
		10	3.5	A	15	-	-	-	70
259	Temperature	0	12	-	25	SS	B	100	-
		0	12	-	25	SS	C	100	-
		7.5	0	A	15	SS	C	100	-
		7.5	0	A	15	CU	C	80	-
		10	3.5	A	-	SS	B	-	-
		10	3.5	A	-	SS	C	-	-
	Radiant Intensity	13	0	A	25	SS	C	-	-
		13	0	A	25	CU	C	-	-
		13	0	B	25	SS	C	80	-
		13	0	B	25	CU	C	80	-
		13	0	B	25	CU	C	80	-
		10	3.5	A	25	-	-	-	70

* Head-on to flow
** An error in the calibration of this instrument that resulted in low values was recently discovered. The correction factor has not yet been evaluated.

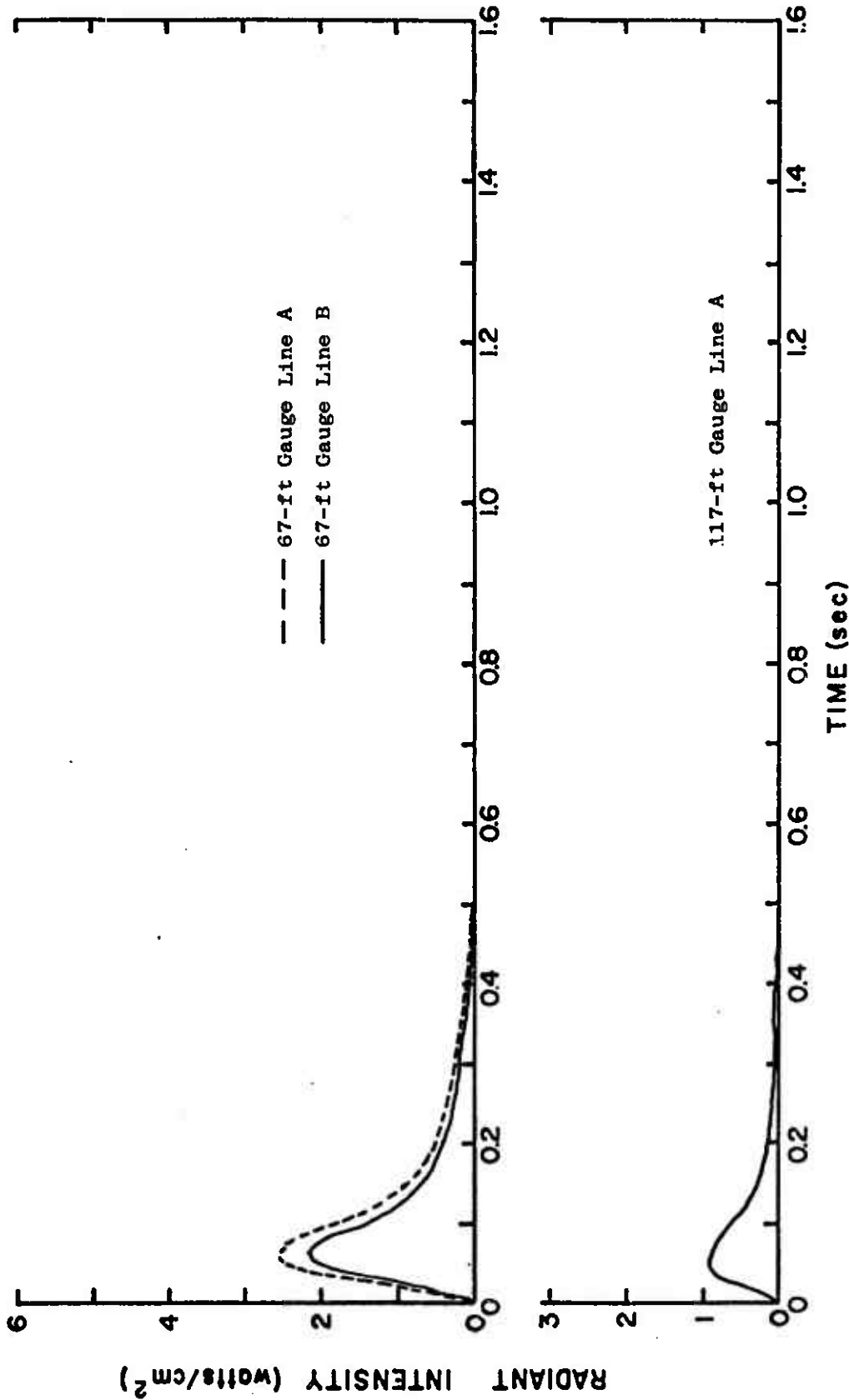


Fig. 23. Radiant Intensity vs Time at Locations Outside the Fireball from Test 243

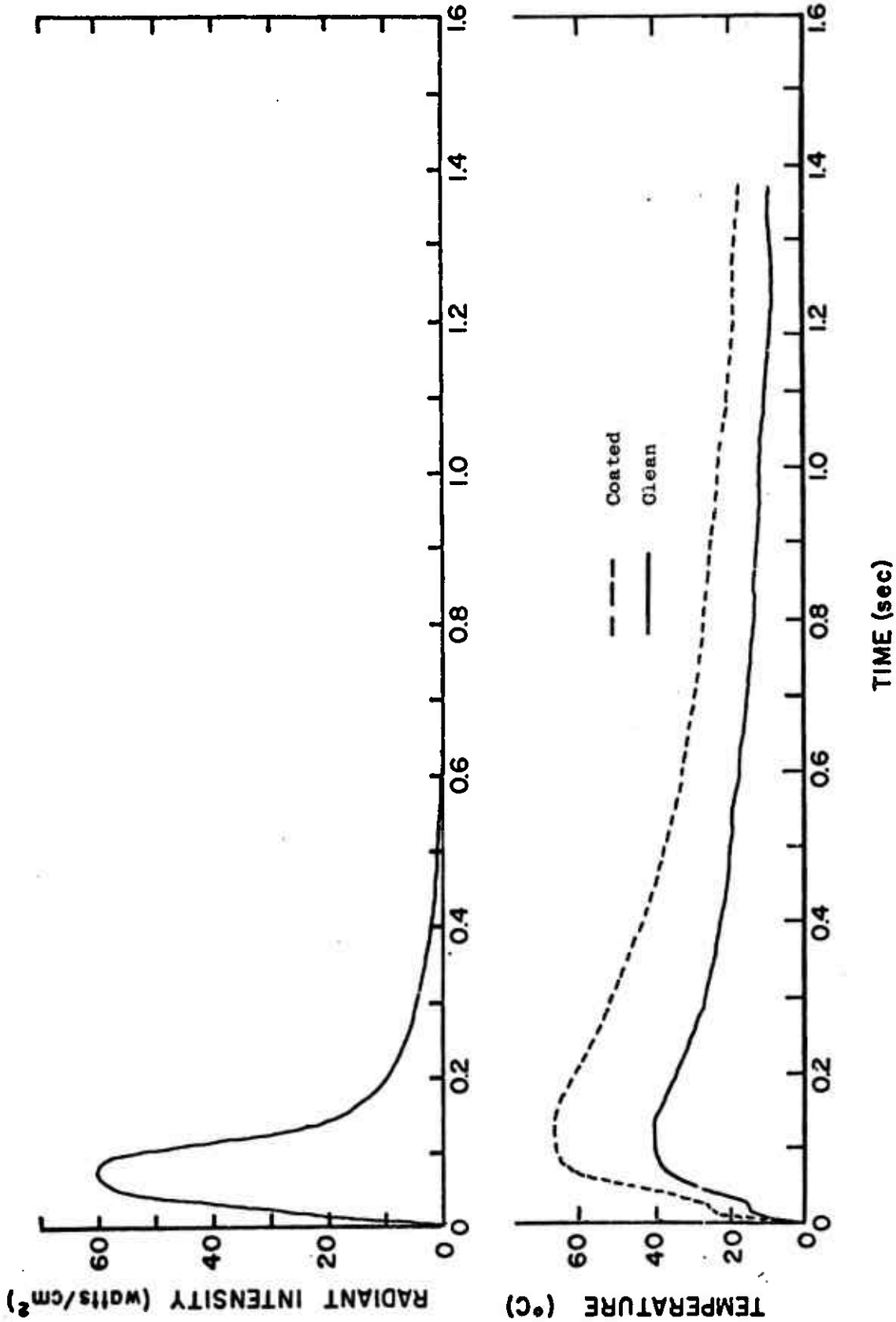


Fig. 24. Stainless Steel Slab Surface Temperature and Radiant Intensity Located 10 ft from Ground Zero Along Gauge Line A for Test 243

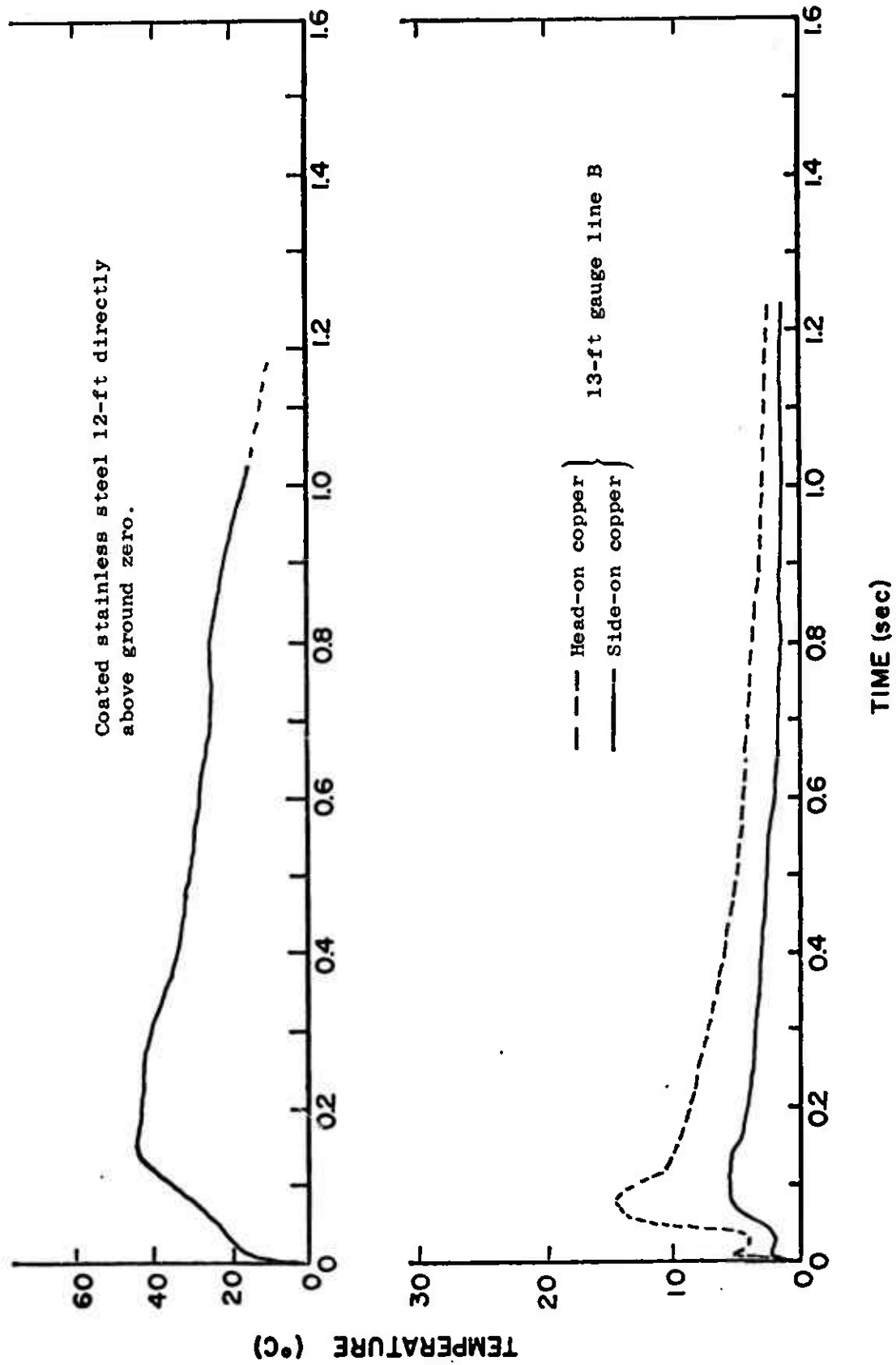


Fig. 25. Slab Surface Temperature for Test 243

The thermal response is exceedingly low for Tests 244 (where the N_2O_4 was above the solid propellant and immediately below the donor charge) and 241 (where the solid propellant was absent and the N_2O_4 replaced by water), and to the limited extent that it could be discerned, data from the two tests were similar in magnitude and duration. A similarity is not surprising since for Test 244 little, if any, of the solid propellant reacted, approximately 90 percent of the solid propellant being recovered.* From high-speed films, evidence of a region of explosive or burning activity subsided after approximately 70 msec for both tests.

In Tests 243 and 259 where the solid propellant was above the N_2O_4 and immediately below the donor charge, the response from each test was similar and somewhat larger in magnitude and duration than for Tests 241 and 244. No solid propellant was found after the tests and evidence of explosive or burning activity subsided after about 350 msec.

One further point about the data should be made. The total energy per unit area per unit time entering a slab may be calculated at any instant from the surface temperature-time trace. This is usually a rather extensive computation and thought to be unwarranted for these data. However, for temperature traces that for a period approximate any of a particular set of mathematically simple forms, an estimate of the heat transfer rate may be readily obtained. Obtaining such an estimate is of interest where radiant intensity and a slab surface temperature have been measured in close proximity since this permits a comparison between the measured rates of radiant and total heat transfer. Estimates of the heat transfer rates to the slabs located 10 ft from ground zero at a height of 3.5 ft for Test 243 give average values over the first 100 msec of 140 and 85 watt/cm² for the black-coated and clean slabs, respectively. As can be seen from a comparison with the radiant intensity measurement at the same location (Table 10 or Fig. 24) where a peak of 60 watts/cm² was obtained, radiant intensity measurements do not account for heat transfer rates necessary to obtain the observed surface temperatures. This difference is accounted for in two ways. First, there is,

* While a container of hydrazine was present, thereby permitting a hydrazine - N_2O_4 reaction, the total quantity of hydrazine was only 0.5 lb.

of course, a forced convection component of energy transfer to the slabs and, second, there are energy losses in the radiant intensity measurement through reflection from and absorption in the protective quartz window of the radiometers, losses that have not been corrected for in the radiant intensity data that are presented. Certain auxiliary thermal measurements have been initiated to evaluate independently convective component and radiant intensity corrections (these measurements are discussed in URS 652-22).^{*} At the present time, however, no quantitative statements can be made.

* C. Wilton, Mansfield, J., A. B. Willoughby, Study of Liquid Propellant Blast Hazards, Contract No. AF 04(611)-10739, URS 652-22, Dec. 1966.

Section 5

CTF/PBAN HIGH-VELOCITY-IMPACT-TEST

The CTF/PBAN high-velocity-impact test was also conducted at the Naval Ordnance Test Station (NOTS), China Lake. In this test 200 lb of this propellant combination was propelled down the sled track at approximately 590 fps and allowed to impact into a deep-hole target. The test condition and the instrumentation system were similar to those used for the N_2O_4 /PBAN test series.

The propellants were contained in a 16-in.-diameter aluminum tank with 140 lb of CTF in the front compartment of the tank and the 60 lb of PBAN, which was formed into a 4-in.-thick cylinder, in the rear compartment. A drawing of this tank is shown in Fig. 26. Photographs of this tank in place on the track and of the PBAN propellant are presented in Figs. 27 and 28.

The deep-hole target, pictured in Fig. 29, broke at the location of the plate forming the bottom of the deep hole, and the front part of the target moved forward approximately 10 ft. The metal liner and the rear plate of the hole remained intact, indicating that no propellant was lost out the back of the target. The majority of the solid propellant (approximately 48 lb) was found in two large pieces approximately 350 ft in front of the target and 50 ft north of the sled track.

The peak overpressure and positive-phase-impulse data are presented in Table 10 and the peak overpressure and positive-phase-impulse yields values, expressed in percent of TNT, are presented in Table 11.

It will be noted that the yields at all distances were extremely low, less than 2% for both peak overpressure and positive-phase impulse. This was not too surprising, since most of the solid propellant was recovered after the test.

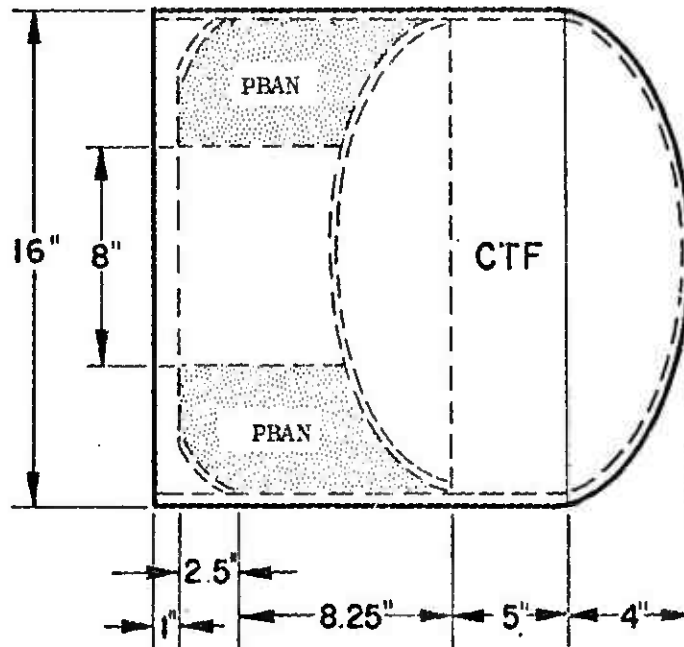


Fig. 26. CTF/PBAN High Velocity Impact Tank.

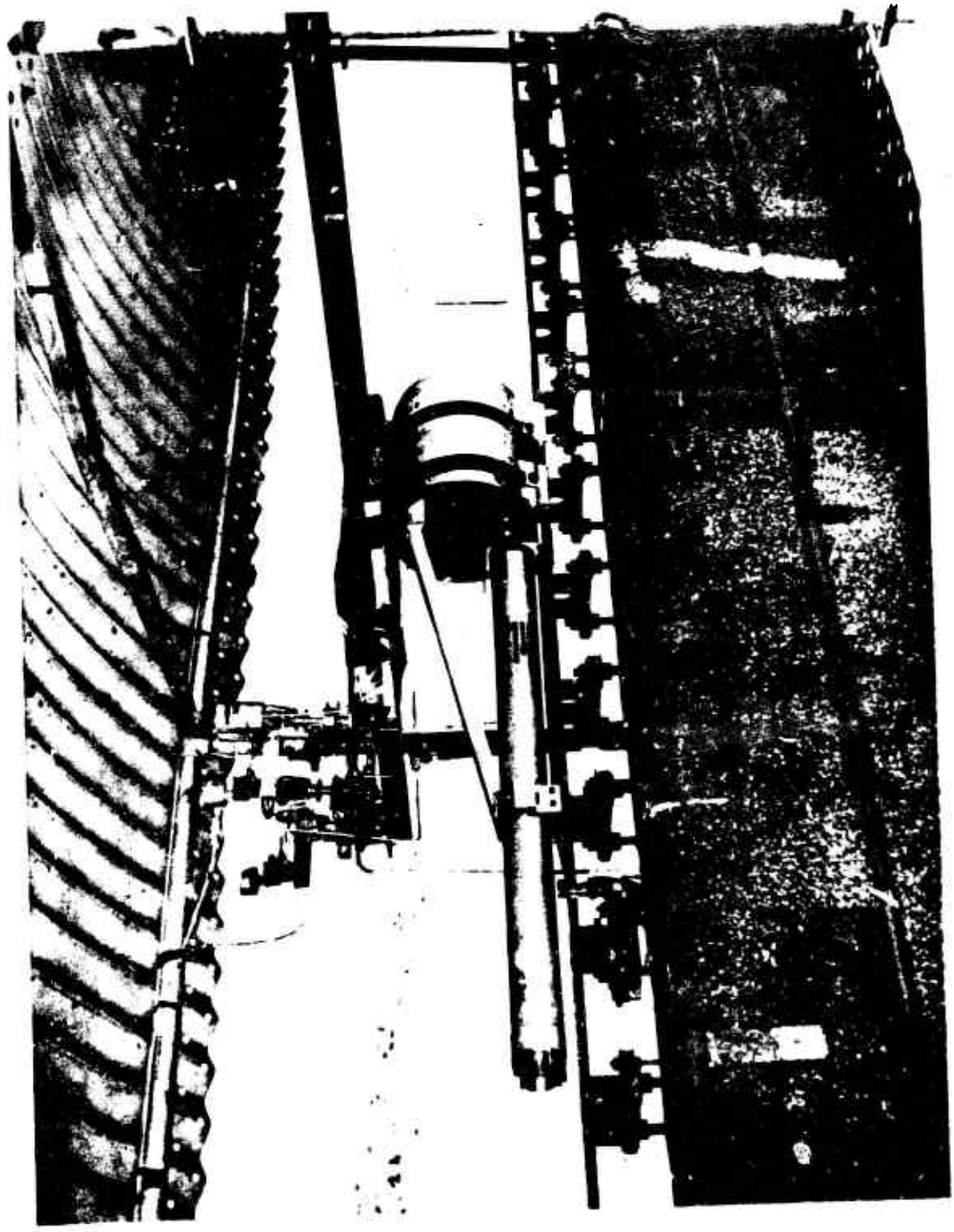


FIG. 27. CTF/PBAN Propellant Tank in Place on Test Track.



Fig. 28. Rear View of CTF/PBAN Propellant Tank Showing PBAN Propellant.



Fig. 29. Post-Shot Photo N_2O_4 /PBAN Deep-Hole Target.

Table 10
PEAK OVERPRESSURE AND POSITIVE-PHASE IMPULSE
DATA FROM CTF/PBAN PROPELLANT TEST

GAUGE LINE	GAUGE	GROUND DISTANCE (ft)	PEAK OVERPRESSURE (psi)	POSITIVE-PHASE IMPULSE (psi/msec)
30-deg	A	21.6	4.8	9.4
	B	33.5	1.8	3.0
	C	64.7	0.6	1.4
	D	115.6	0.4	0.1
90-deg	B	37.7	0.8	2.0
	C	65.5	0.4	1.0
	D	117.	0.2	0.5
180-deg	D	117.5	0.1	0.2

Table 11
EXPLOSIVE YIELDS FROM CTF/PBAN HIGH-VELOCITY-IMPACT TEST
ADJUSTED TO TNT

GAUGE LINE	GAUGE	GROUND DISTANCE (FT)	PEAK OVERPRESSURE YIELD (%)	POSITIVE-PHASE IMPULSE YIELD (%)
30 deg	A	21.6	1.3	2.2
	B	33.5	0.7	0.7
	C	64.7	0.5	0.5
90 deg	B	37.7	0.2	0.4
	C	65.5	0.2	0.3
	D	117	0.3	0.2
180 deg	D	117.5	0.1	0.1

The best estimate of terminal yield for this test is 0.6%. This value was obtained by averaging the terminal yield in the 0-, 90-, and 180-deg directions, with the 0-deg direction obtained by extrapolation. For a complete discussion of the rationale behind this method of determining terminal yield, see Section 4.

Section 6
DISCUSSION OF RESULTS

N_2O_4 /PBAN TESTS

The terminal yield results from the hybrid tests series are given in Table 12. As expected, the tower drop test condition gave the lowest yield values. In fact, the values were so low that no measurable deflections were obtained on the pressure records and only estimates of the upper bounds on the yield values could be obtained. It is quite likely that no explosion occurred, since observers in the blockhouse did not detect any sound from the tests.

The high-velocity impact tests gave intermediate yield values ranging from 0.3% for the flat-wall target to as high as 3.7% for one of the two tests using the deep-hole target. The higher values for the deep-hole case are consistent with previous results obtained for the hypergolic and cryogenic propellants and are attributed to confinement effects.

The 30-lb explosive-donor tests gave the highest yield values. For the tank configuration with the solid on top, yield values were 10 and 15% and with the liquid on top, about 5%. The greater yield values for the former case are not surprising because in this case the explosive donor first shatters the solid fuel and then drives it into the liquid, seemingly an ideal way to mix the propellants. In the latter case, with the liquid on top, less breakup and dispersal of the solid fuel (90% recovered) would be expected because of the attenuation of the shock in the liquid propellant.

It should be kept in mind that although significant yields (5 to 15%) were obtained for the explosive-donor tests, even the largest of these obtained, 15%, was only equal to the weight of the explosive donor, 30 lb, and the other two were one-third to one-half its weight.

CTF/PBAN TEST

The terminal yield for the single deep-hole-target CTF/PBAN test was

Table 12
SUMMARY OF TERMINAL YIELDS FROM N_2O_4 /PBAN TESTS

TEST CONDITION	TERMINAL EXPLOSIVE YIELD (% of TNT)
HIGH-VELOCITY IMPACT	
Flat Wall	0.3
Deep Hole	1.0, 3.7
EXPLOSIVE DONOR	
Liquid Over Solid	5
Solid Over Liquid	10, 15
TOWER DROP	
2 Tests	< 0.01

approximately 0.6%, which is somewhat greater than the yield from the flat-wall test and less than the yield from the deep-hole test for the N_2O_4 /PBAN propellant combination.

COMPARISON WITH HYPERGOLIC RESULTS

As a matter of interest, the explosive yield values from the hybrid tests are compared with the results obtained from the N_2O_4 /50-50 propellant combination in Table 13. It can be seen that for the high-velocity-impact and tower-drop cases, the hybrid yields are significantly less than those from the hypergolic combination. For the explosive-donor case, however, the hybrid yields tend to be larger, particularly for the tank configuration with the solid on top.

Table 13
 COMPARISON OF HYBRID AND HYPERGOLIC TERMINAL YIELDS
 (200-lb scale)

TEST CONDITION	TERMINAL EXPLOSIVE YIELD (% of TNT)		
	N ₂ O ₄ /PBAN	CTF/PBAN	HYPERGOLIC
HIGH-VELOCITY IMPACT			
Flat Wall	0.4	-	13, 15
Deep Hole	1.4, 4.3	0.6	56, 37
EXPLOSIVE DONOR			
Liquid Over Solid	4.7	-	3.4, 3.7
Solid Over Liquid	8.7, 12.6	-	
TOWER DROP	< 0.01	-	0.3, 0.3, 0.3

APPENDIX A*
DESCRIPTION OF N₂O₄/PBAN TESTS

Presented in this appendix are brief descriptions of each of the N₂O₄/PBAN tests, photographs of the test facilities and test hardware, pretest and post-test photographs of some of the high-explosive calibration tests, and pre-test and post-test photographs for the majority of the propellant tests.

HIGH-VELOCITY-IMPACT TEST SERIES

The high-velocity-impact test series was conducted at the Naval Ordnance Test Station, China Lake, on the K-2 Terminal Ballistic Range. A schematic of this facility is shown in Fig. A-1. A photograph of the Hybrid Test Article in position on the sled track is shown in Figs. A-2 and A-3.

The impact targets used for this test series were a flat-wall target, shown in Fig. A-4, and a deep-hole target, shown in Fig. A-5.

Brief descriptions of each of the calibration tests and the high-velocity-impact tests are presented in chronological order below.

- Test No. 1: 8-lb TNT block detonated at a position 3 ft from the ground and 1 ft from the 4-in.-thick steel plate. This was an air blast instrumentation functional test.
- Test No. 2: 18-lb pentolite sphere (Fig. A-6) detonated at a position 3 ft from the ground and 1 ft from the 4-in.-thick steel plate. This was an air blast instrumentation calibration test.

* This appendix prepared by

Austin A. Dickinson
Project Engineer, Hybrid Hazard Program
Hazards Analysis Branch
Solid Rocket Division
Air Force Rocket Propulsion Laboratory

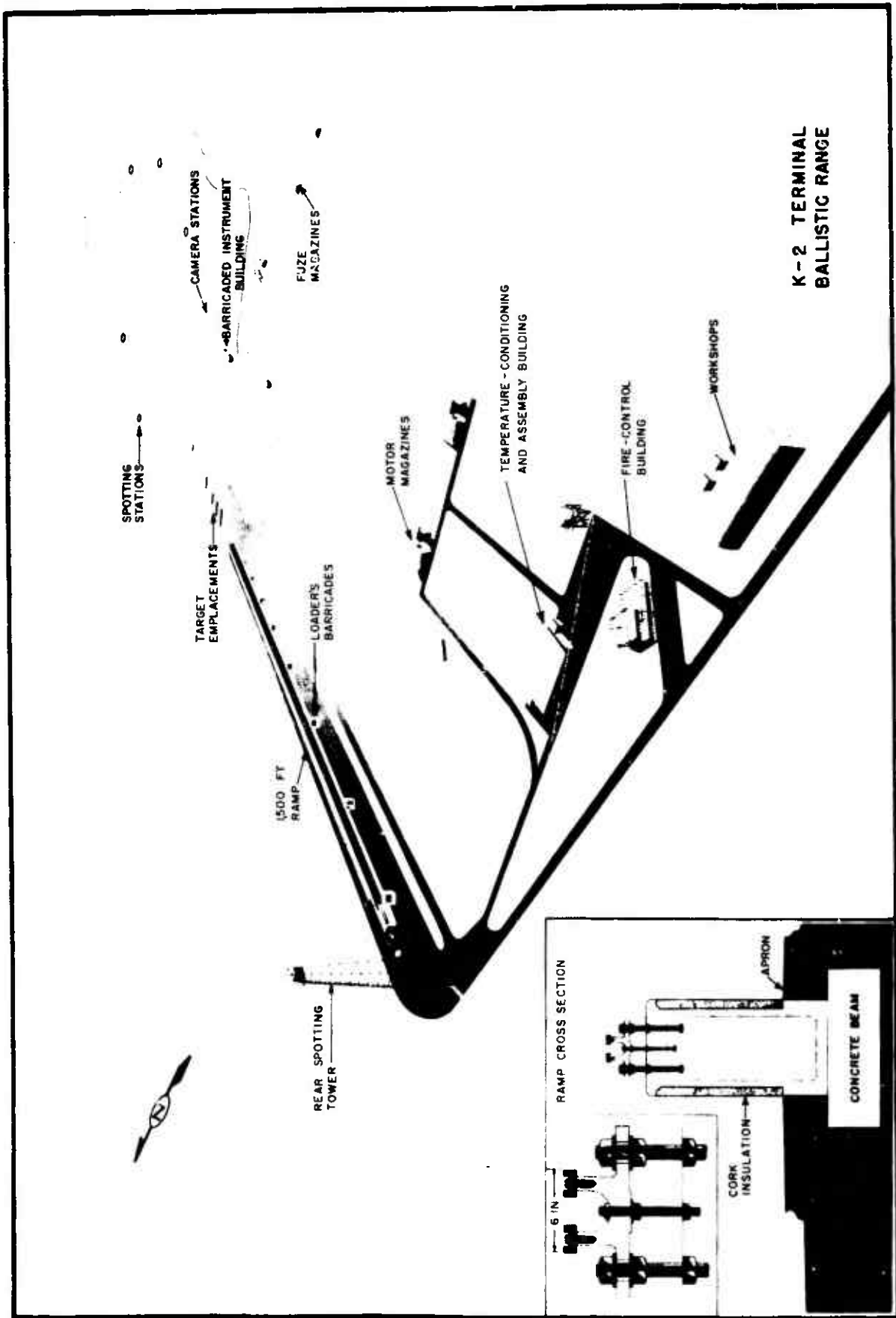


Fig. A-1. Schematic of K-2 Terminal Ballistic Range

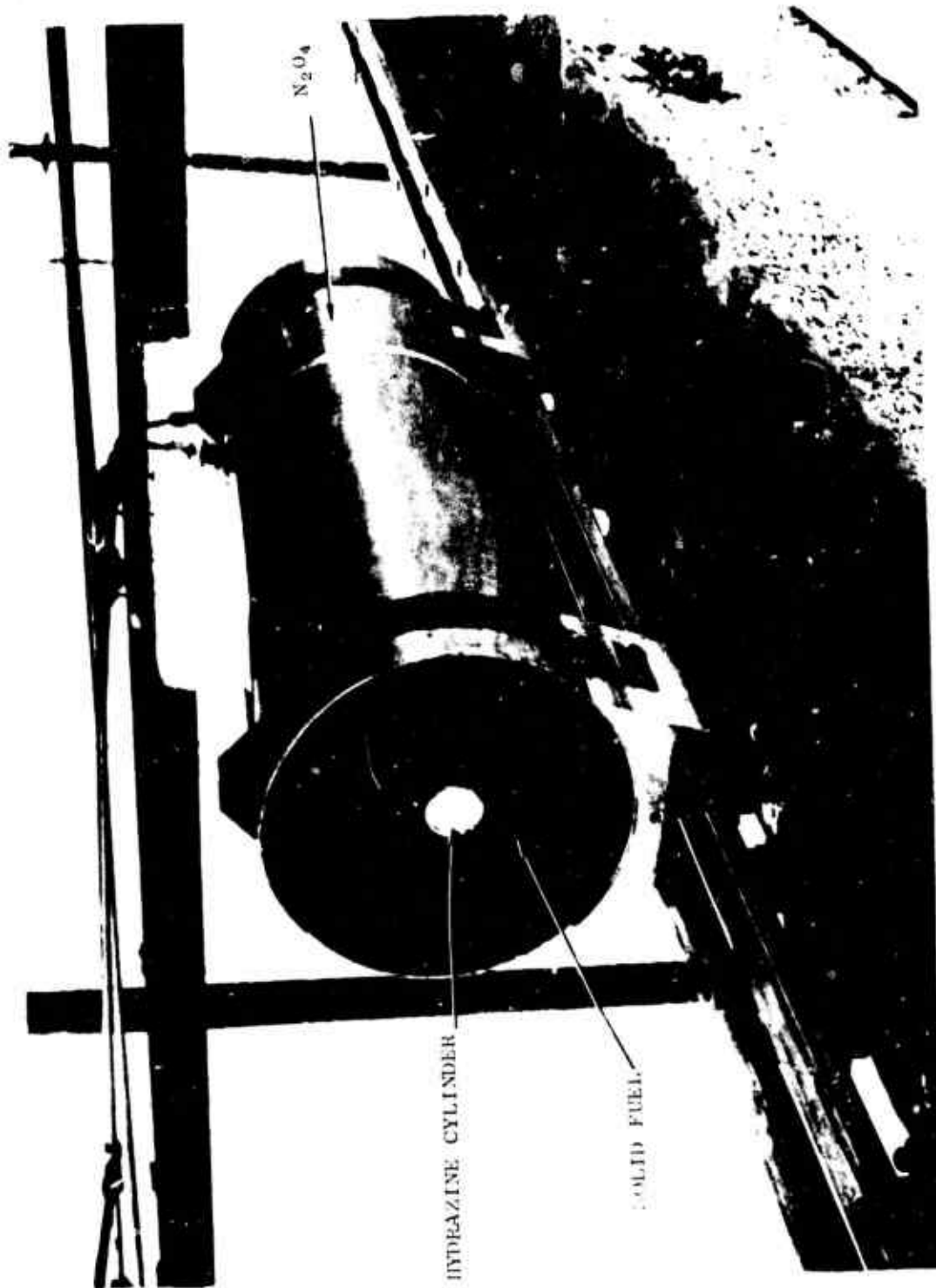


Fig. A-2. N_2O_4 /PBAN High-Velocity-Impact Tank

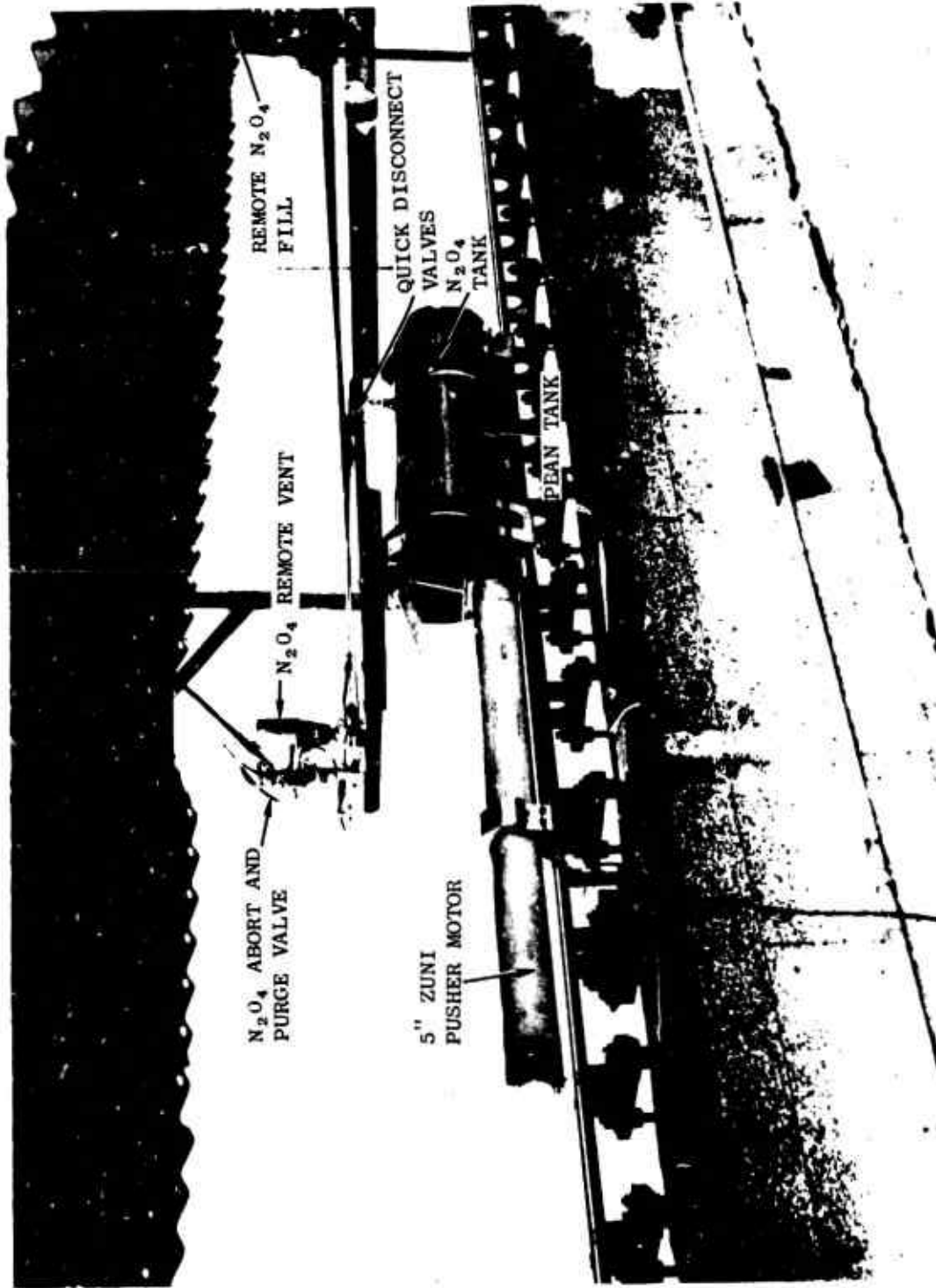


Fig. A-3. N_2O_4 /PBAN High-Velocity-Impact Tank and Propulsion Unit.



Fig. A-4. Flat-Wall Target.



Fig. A-5. Deep-Hole Target.



Fig. A-6. Pre-Test Photo, Test Number 2.

- Test No. 3: Propellant impact test into a deep-hole target at a velocity of 691.8 ft/sec.* No damage was done to the target (Fig. A-7). Approximately 20 lb of solid fuel were recovered within 50 ft of the target. A small amount (about 10 lb) of solid fuel was recovered between 50 ft and 400 ft.
- Test No. 4: Impact onto a flat-wall target at a velocity of 591.7 fps.* No damage to the target (Fig. A-8). Approximately 40 lb of the solid fuel were recovered within a 400-ft radius of the target. A small amount of this could be from the previous test.
- Test No. 5: Impact into a deep-hole target at a velocity of 586.8 fps.* No damage to the target (Fig. A-9). Approximately 30 lb of solid fuel were recovered within a 400-ft radius of the target.
- Test No. 6: 8-lb TNT block detonated against the center of the back of a deep-hole target (Fig. A-10). This was an instrumentation functional test.
- Test No. 7: 18-lb pentolite sphere detonated against the center of the back of a deep hole target (Fig. A-11). This was an instrumentation calibration test. The target sustained extensive damage. The concrete spalled away from both sides and the top to a depth of 1 ft (Fig. A-12).

EXPLOSIVE-DONOR AND DROP-TEST SERIES

The explosive donor and the drop test series were conducted at the Air Force Rocket Propulsion Laboratory, Edwards, California, on the Liquid Propellant Blast Hazard Program (Project PYRO) Test Stand. A photograph of this test stand and the 100-ft drop tower is shown in Fig. A-13.

Brief descriptions of each of the calibration tests, explosive-donor tests and drop tests are presented in chronological order below:

- Test No. 241: Explosive donor using a 30-lb composition B charge on a hybrid tank filled with water.

* Note that the impact velocity for Test No. 3 was about 100 fps higher than for Tests 4 and 5. The only explanation that can be offered for this increased velocity is that the track was cleaned with kerosene prior to this test and the resulting film on the track for the first test could have acted as a lubricant not present for the next two tests.

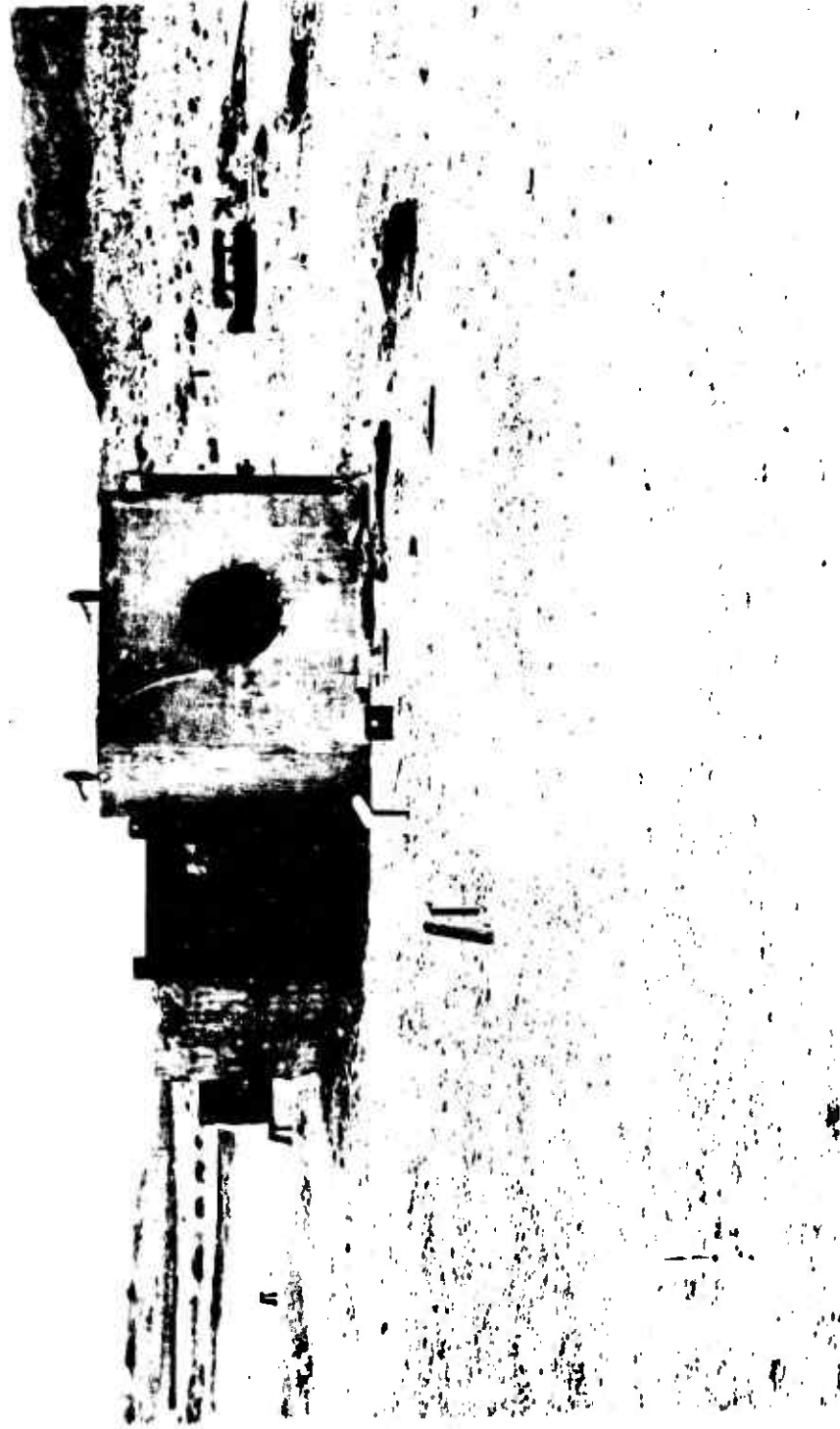


Fig. A -7. Post-Test Photo, Test Number 3

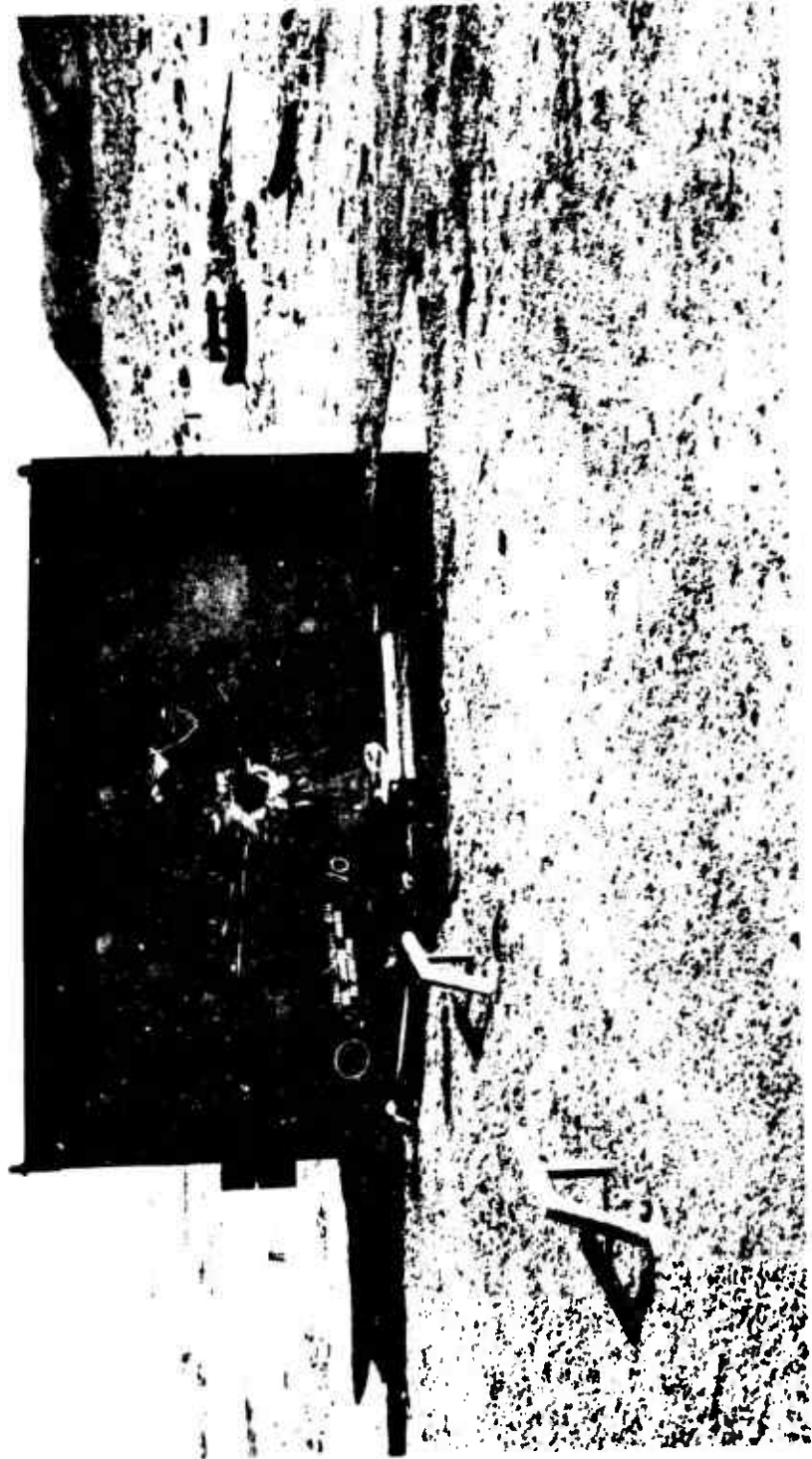


Fig. A-8. Post-Test Photo, Test Number 4

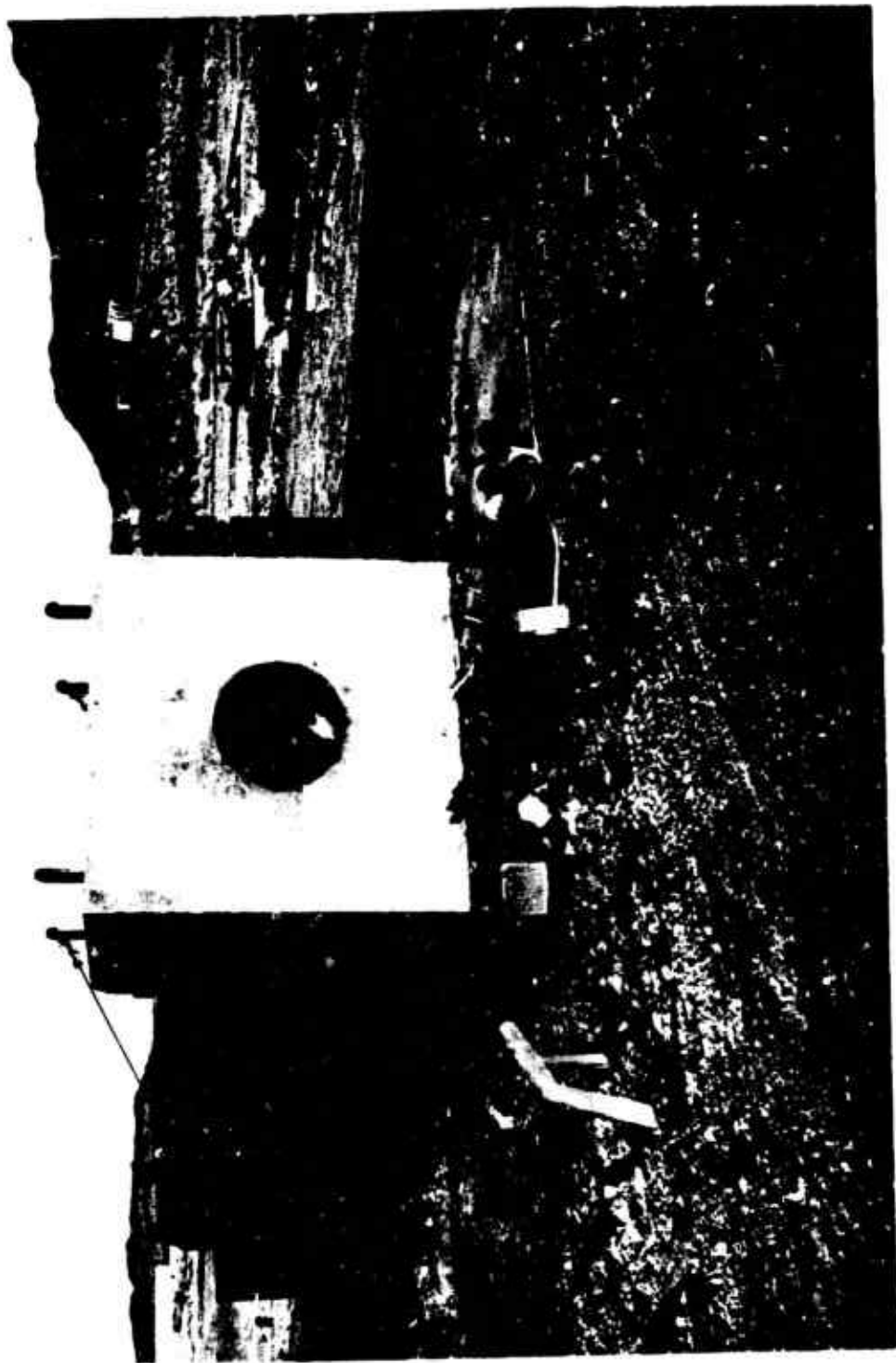


Fig. A-9. Post-Test Photo, Test Number 5.

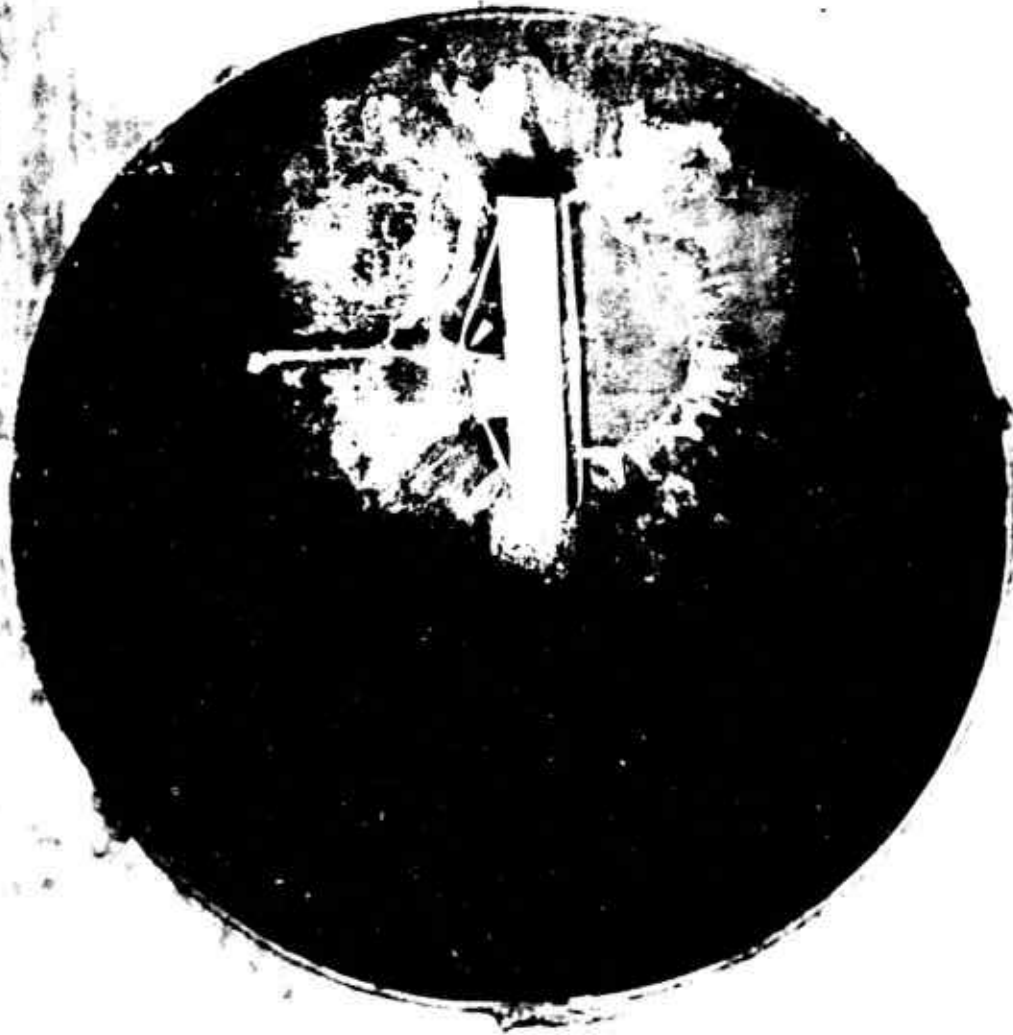


Fig. A-10. Pre-Test Photo, Test Number 6.

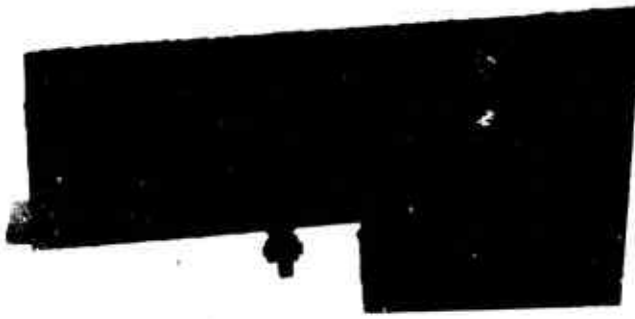


Fig. A-11. Pre-Test Photo, Test Number 7.



Fig. A-12. Post-Test Photo, Test Number 7.

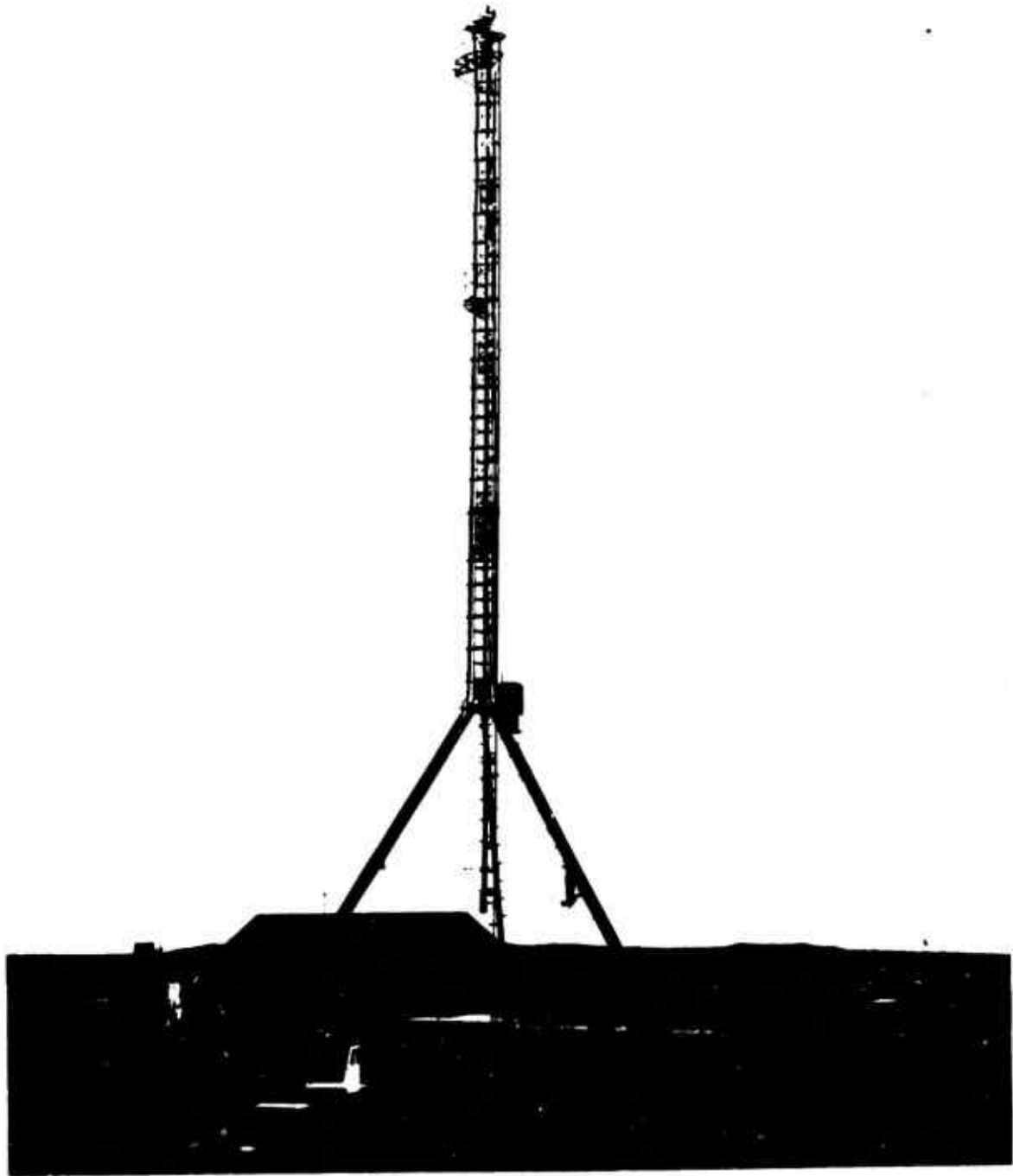


Fig. A-13. Liquid Propellant Hazard Test Stand and Tower

- Test No. 243: Explosive-donored test with PBAN in the top tank and N_2O_4 in the bottom tank (Fig. A-14). The N_2H_4 cylinder was placed in the center core of the PBAN. The solid fuel was entirely consumed in this test and tank fragments were found from 0 to 100 ft from the test stand.
- Test No. 244: Explosive donored test with N_2O_4 in the top tank and PBAN in the bottom tank (Fig. A-15). The N_2H_4 cylinder was placed in the center core of the PBAN. Approximately 90% of the solid fuel was recovered after this test. Tank fragments were found from 0 to 50 ft from the test stand (Fig. A-16).
- Test No. 259: Explosive-donored test with PBAN in the top tank and N_2O_4 in the bottom tank. The N_2H_4 cylinder was placed in the center core of the PBAN. The solid fuel was entirely consumed in this test and tank fragments were found from 0 to 100 ft from the test stand.
- Test No. 260: High drop test with PBAN in top tank and N_2O_4 in the bottom tank (Fig. A-17). The N_2H_4 cylinder was placed in the center core of the solid fuel. Impact velocity was 75 fps. The N_2O_4 tank ruptured on impact. As can be seen in Figs. A-17 and A-19, the solid tank was only slightly damaged and no fire was started. The N_2H_4 cylinder was recovered intact.
- Test No. 261: High drop test with N_2O_4 in the top tank and PBAN in the bottom tank (Fig. A-20). The N_2H_4 cylinder was placed in the center core of the PBAN. Impact velocity was 75 fps. On impact, the aluminum diaphragm was ruptured, and N_2O_4 escaped through the solid fuel core (Figs. A-21, A-22, and A-23). The top of the N_2O_4 tank was ruptured, and a jet of N_2O_4 could be seen rising above the rest of the N_2O_4 cloud in a straight column. The N_2H_4 cylinder was crushed and a lazy fire started. Damage to the solid fuel tank was slight and the fuel segment was intact.

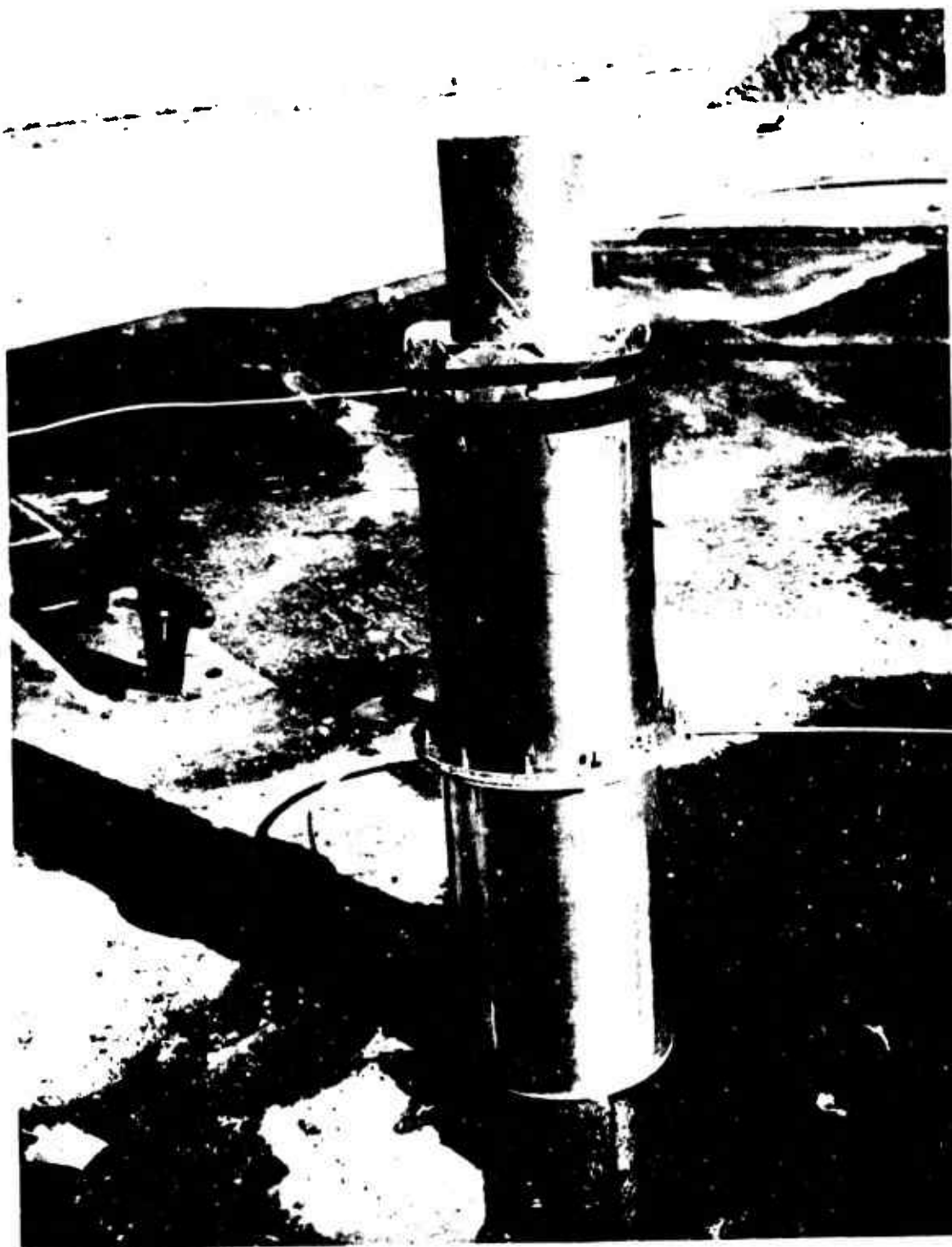


Fig. A-14. Pre-test Photo, Test Number 243

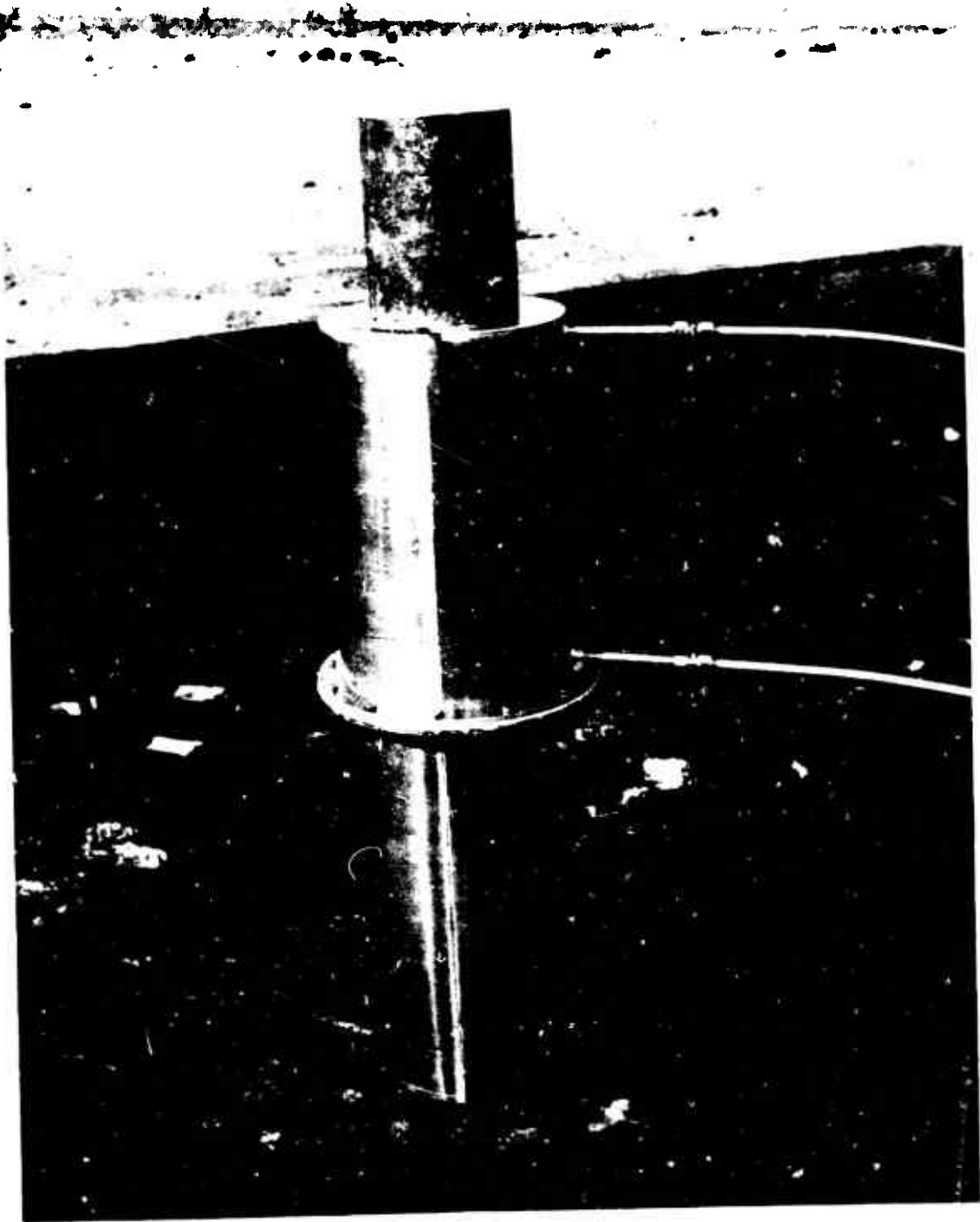


Fig. A-15. Pre-Test Photo, Test Number 244.



Fig. A-16. Post-Test Photo, Test Number 244.



Fig. A-17. Pre-Test Photo of Test of Test Article Used for Test Number 260.



Fig. A-18. Post-Test Photo, Test Number 260.



Fig. A-19. Post-Test Photo, Test Number 260.

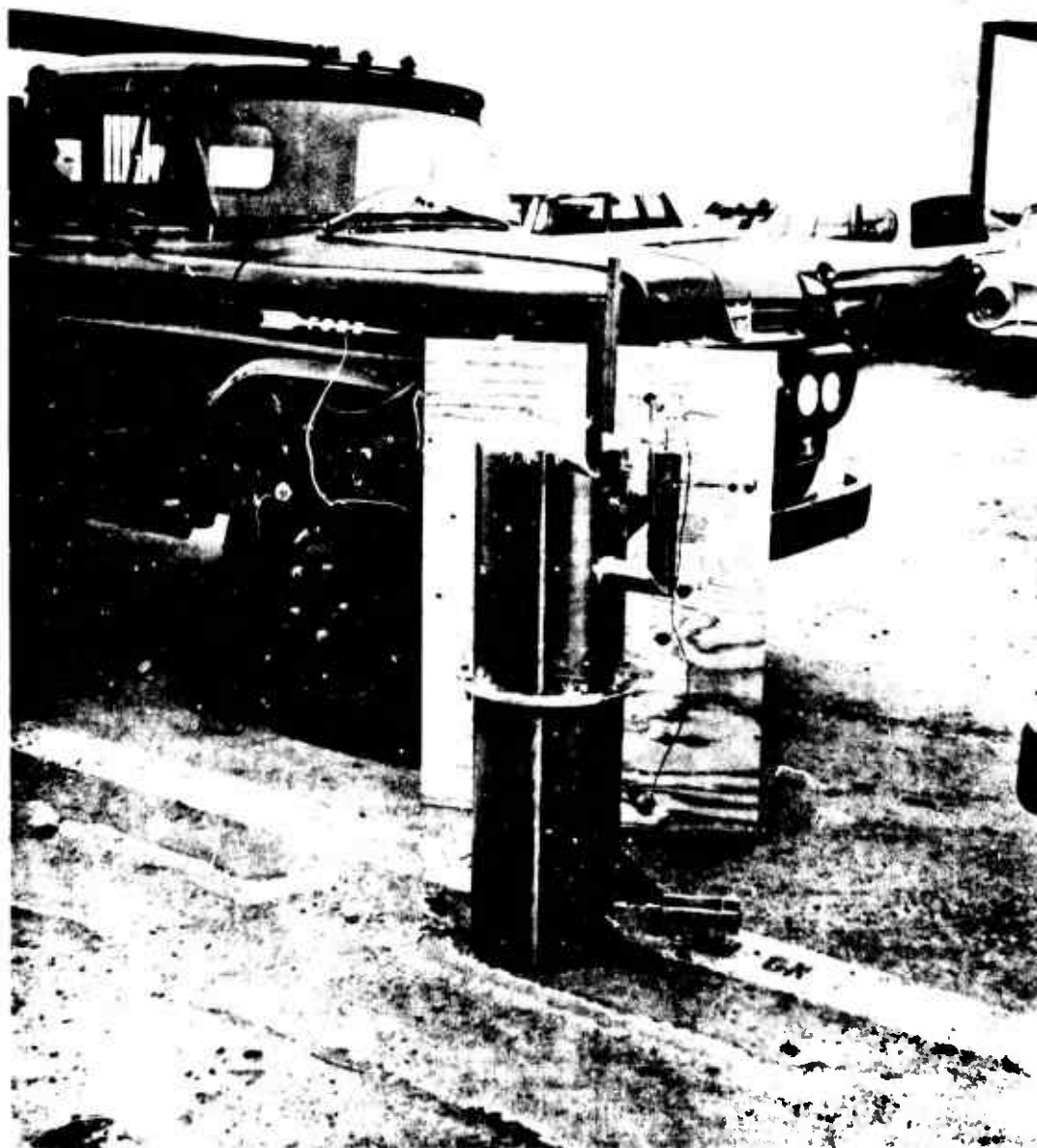


Fig. A-20. Test Article used for Test Number 261.



FIG. A-21. Post-Test Photo, Test Number 261.



Fig. A-22. Post-Test Photo, Test Number 261.



Fig. A-23. Post-Test Photo, Test Number 261.